THESIS FOR THE DEGREE OF LICENTIATE OF ENGINEERING

Dynamics of large-scale fluidized bed combustion plants

Modeling, simulation and control

GUILLERMO MARTINEZ CASTILLA

Department of Space, Earth and Environment

CHALMERS UNIVERSITY OF TECHNOLOGY

Gothenburg, Sweden 2021

Dynamics of large-scale fluidized bed combustion plants
Modeling, simulation and control

GUILLERMO MARTINEZ CASTILLA

Department of Space, Earth and Environment
Chalmers University of Technology
SE-412 96 Gothenburg
Sweden
Telephone +46(0)31-772 1000

Printed by Chalmers Reproservice
Gothenburg, Sweden 2021

Dynamics of large-scale fluidized bed combustion plants

Modeling, simulation and control

GUILLERMO MARTINEZ CASTILLA
Division of Energy Technology
Department of Space, Earth and Environment
Chalmers University of Technology

Abstract

Fluidized bed combustion (FBC) plants are widely used in energy systems across the world for the thermochemical conversion of solid fuels, and are especially suitable for low-rank fuels (a category to which renewable solid fuels belong). FBC plants are traditionally operated for base-load electricity production and for heat production, both of which processes are characterized by steady and stable operation. As the share of variable renewable electricity (VRE) sources is expected to increase dramatically, FBC plants will have to adapt their operations to the new flexibility requirements related to the inherent variability of VRE sources. By enhancing their operational and product flexibilities, FBC plants can remain financially attractive and offer services to support the balancing of the grid. As tools for assessing the operational flexibility of thermal power plants, dynamic modeling and simulation are gaining attention from both researchers and plant operators. However, it is a common practice to assume that the dynamics of the gas side are much faster than those of the water-steam side, i.e., not accounting for the in-furnace dynamic mechanisms.

This thesis aims to characterize the dynamic behaviors of commercial-scale FBC plants, accounting for both the gas and water-steam sides of bubbling and circulating fluidized bed (BFB and CFB) units. For this purpose, a dynamic semiempirical model of the gas side of FBC plants is developed and integrated into a process model of the water-steam side. The models are validated against steady-state and transient operational data measured at two commercial-scale industrial units. The model is then used to analyze the inherent dynamics of the gas and water-steam sides, to compare the transient behaviors of BFB and CFB units, and to assess the dynamic performances of FBC plants when operated under different control structures.

The results of the dynamic analysis show that the stabilization times of the temperatures across the furnace differ, largely based on the local heat capacity of the region in the furnace, i.e., the amount of bulk solids. The work includes an assessment of the impact of the characteristic times of the in-furnace mechanisms (i.e., fluid dynamics, fuel conversion and heat transfer) on the computed stabilization times of key in-furnace variables at plant level, and suggests some simple mathematical relationships for predicting these times. When accounting for the water-steam side, the results show that the inherent dynamics of variables such as live steam pressure, flow and power production are in the same order of magnitude as the dynamics of the gas side, particularly for the CFB case. This highlights the importance of accounting for the gas side when attempting to model accurately the dynamics of FBC plants. Furthermore, FBC plants are found to be able to provide fast load changes when operated under control structures that manipulate the live steam valve, although this is found to trigger operational issues, such as pressure overshoots.

The results of this thesis are of particular importance in terms of assessing the transient capabilities of FBC plants to operate in electricity-driven markets where fast operation is

required, and they can be used to identify opportunities and challenges. Furthermore, knowledge about the transient operation of large-scale FB reactors will be crucial for the development of FB applications other than combustion, such as polygeneration or thermochemical energy storage.

Keywords: operational flexibility, thermal power plant, process control, combined heat and power, biomass combustion

List of publications

The thesis is based on the following appended papers, which are referred to in the text by their assigned Roman numerals:

I. G.M.Castilla, R.M. Montañés, D. Pallarès and F. Johnsson.
"Dynamic modeling of the reactive side in large-scale fluidized bed boilers".
Industrial and Engineering Chemistry Research, **2021,** 60, 3936-3956.

II. G.M.Castilla, R.M. Montañés, D. Pallarès and F. Johnsson.
"Comparison of the transient behaviours of bubbling and circulating fluidized bed combustors".
Submitted for publication, **2021**

III. G.M.Castilla, R.M. Montañés, D. Pallarès and F. Johnsson
"Transient operation capabilities of biomass-fired fluidized bed combined heat and power plants. Dynamic modeling and control".
To be submitted, **2021**

Guillermo Martinez Castilla is the principal author of **Papers I – III** and performed the modelling and analysis for all three papers. Rubén M. Montañés contributed to the method development in **Papers I-III** as well as with editing and discussion for all three papers. Associate Professor David Pallarès contributed to the method development in **Papers I-III**, as well as with editing and discussion for all three papers. Professor Filip Johnsson contributed with discussion and editing in **Papers I-III**.

Other publications by the author, not included in the thesis:

- G. M. Castilla, M. Biermann, R.M. Montañés, F. Normann and F. Johnsson. "Integrating carbon capture into an industrial combined-heat-and-power plant: performance with hourly and seasonal load changes". *International Journal of Greenhouse Gas Control*, **2019,** 82, 192-203.

- G. M. Castilla, A. Larsson, L. Lundberg, F. Johnsson and D. Pallarès. "A novel experimental method for determining lateral mixing of solids in fluidized beds – Quantification of the splash-zone contribution". *Powder Technology*, **2020,** 370, 96-103.

- G. M. Castilla, D.C. Guío-Pérez, S. Papadokonstantakis, D. Pallarès and F. Johnsson. "Techno-economic assessment of calcium looping for thermochemical energy storage with CO_2 capture". *Energies*, **2021,** 14, 3211

- G. M. Castilla, R.M. Montañés, D. Pallarès and F. Johnsson. "Dynamic modeling of the flue gas side of large-scale circulating fluidized bed boilers". *In proceedings of CFB-13 conference*, Vancouver, Canada, **2021**

Acknowledgements

I would like to start by thanking my supervisors: each of them has been a key piece for the development of this work. Working with 4 supervisors is a continuous learning for which I am thankful every single day. First of all, David, thank you for being a steady light glowing through the dark winters. Not only your knowledge and dedication are precious, I also truly appreciate our abundant non-work conversations, from music and sports to travelling and literature. Rubén, infinite thanks for your support, hours-long discussions, brainstorming, inspiration and many more. It has been now more than three years working back to back, and only you know how important your presence is for me, and for this work. Filip, thank you for always finding the time and energy to bring up new ideas, perspectives, and discussions. Your time management is something that truly fascinates me and learning from you is very inspiring. Last but not least, thank you Carolina for moving to Gothenburg in the middle of a global pandemic and joining the team. In only one year I have already learnt lots from you and I can´t wait for all the discussions ahead of us!

My gratitude goes also to my examiner Henrik Thunman, whose busy office has always been open for me. Very special thanks to Fredrik, Max and Stavros for opening me the doors of the division three and a half years ago and initiating this longer-than-expected adventure.

Thank you Bioshare for a great collaboration and useful discussions, all the luck for all the exciting projects you have ahead! Thanks also to Karlstad and Övik Energi for an impressive work answering to all our requests.

Co-workers of Energy Technology: thanks to all of you for contributing to create the fantastic workplace we have. With this regard, special mention to Marie and Katarina for their everlasting good and helping mood we all should learn from. Thanks to my PhD colleagues (some of you now friends) for lunches, walks, afterwork sessions, board games, volleyball and more. Sharing this adventure with you all is crucial for me. Special thanks also to my office mate Tove: I wish you all the best in the future! To the newly born Fluidization group, thanks for our Monday meetings and the space for sharing and discussing that we have created in this short time.

I would not be the person I am without my friends. Thank you Guarida for that. Also big thanks to my friends in Gothenburg and Iceland for being my family far from home

Lastly, I would like to thank my family for making all this possible. I can feel your love and support no matter where we are. Stef, it is a real joy to walk next to you day after day, alltaf. Thanks for continuously teaching me about the things that really matter in life.

This work has been financed by the Swedish Energy Agency under the project “Cost-effective and flexible polygeneration units for maximized plant use” (P-46459-1).

Guillermo Martinez,
Majorna, May 2021

“If we take care of the moments, the years will take care of themselves”

- Maria Edgeworth

Table of Contents

Nomenclature and terminology

Latin symbols

A: area
a: decay factor
C: controller
c: concentration, heat capacity
D: diameter
F: flow,
h: heat transfer coefficient
I: instrument
K: transport decay factor, backflow effect ratio, flow area coefficient
k: decay constant, absorption coefficient
L: level, lenght
M: total mass
P: pressure instrument
p: pressure
Q: heat flow, composition,
R: reading
St: stokes number
T: temperature, transmitter,
t: time
u: velocity
y: process variable

Greek symbols

τ: characteristic time
η: efficiency
ε: voidage
σ: Stefan-Boltzmann constant
ρ: density

Subscripts

b: backflow
c: convection, core
comb: combustion
db: dense bed
DH, in: inlet district heating water
DH, out: outlet district heating water
e: equivalent
el: electricity
entr: entrained
extracted, i: extracted in a certain cell *i*
f: fuel
g: gas

in: inlet
n: nominal
p: particle, at constant pressure
rad: radiation
s: stabilization
susp: gas-solid suspension
t: terminal, turbine
top: at furnace top
vol: volumetric
w: wall
Walls: to the waterwalls
wl: wall-layer
0: before change is introduced
∞: after new steady-state is reached

Abbreviations

BF: boiler-following
BFB: bubbling fluidized bed
CFB: circulating fluidized bed
CHP: combined heat and power
CP: centrifugal pump
DH: district heating
DHC: district heating condenser
DSH: desuperheater
ECO: economizer
FB: fluidized bed
FBC: fluidized bed combustion / combustor
FC: fuel conversion
FD: fluid dynamics
FG: flue gas
FP: floating pressure
FWH: feedwater heater
HHV: high heating value
HPT: high pressure turbine
HT: heat transfer
IPCD: integrated process control design
IPT: intermedium pressure turbine
LPT: low pressure turbine
MPC: model predictive control
OFWH: open feedwater heater
RC: relative change
SH: superheater
SP: set-point
TF: turbine-following
VRE: variable renewable electricity
VRR: variable ramping rate
TCES: thermochemical energy storage

Glossary

The following terms are recurrent throughout the text:

Controlled dynamics: Transient behavior of the plant/furnace when running with closed (i.e. activated) control loops.

Dynamic analysis: investigation of the different aspects related to the transient operation of FBC plants.

Gas side: Combustion chamber of the furnace in which the fuel, bulk solids and gas are located. In some contexts, also referred as *in-furnace*. Note that the furnace walls and convective flue gas path are in this work considered part of the water-steam side.

Inherent dynamics: Transient behavior of the plant/furnace when running with open (i.e. deactivated) control loops.

Model calibration: Fine-tuning of model parameters to adjust the model output so that it resembles more accurately a specified operational dataset of a certain reference unit.

Model formulation: Writing and balancing of the model, i.e. of the system of equations consisting of mass and heat balances.

Model validation: Use of the calibrated model to predict steady-state and transient operational datasets others than the one used for calibration.

Open-loop: Uncontrolled response of the system variables after a step-change in one of the inputs.

Reference units: Commercial-scale FBC plants used for collecting operational data.

Water-steam side: All the equipment related to the water-steam loop conforming the Rankine cycle, i.e., the convective flue gas path (economizers and superheaters), evaporator tubes and in-furnace walls, steam drum, steam lines and valves, steam turbines, condensers, deaerators, feedwater heaters, pumps and valves.

1. Introduction

In accordance with the Paris Agreement [1], decarbonization of the power sector is a priority to maintain global warming at well below 2°C above pre-industrial levels [2]. Electricity supply from renewable sources such as wind and solar represents a key solution to this challenge [3], and the share of renewable sources in the worldwide electricity generation is expected to increase from 25% in Year 2016 to 33% in Year 2025 on global level, playing a crucial role by Year 2050 in the electricity production of most European countries [4],[5]. However, electricity generated from wind and solar power is subject to weather variations, so it is often referred to as variable renewable electricity (VRE). This intermittency creates a need for power system balancing to ensure security of supply at all times. As the share of VRE generation surges, the variations in the net load curve (calculated by subtracting the renewable energy generation from the total energy demand) increase. This net load is currently met by thermal power plants in most of the energy systems worldwide [6], and the impact of the penetration of VRE on the operational patterns of these plants is already noticeable in some regions [7], as they are operated to provide regulation and back-up capacity to the grid during periods with very low levels of solar and wind power generation [8]. Thus, it is clear that practically all thermal power plants existing and to be commissioned for power production will be required to adapt their operation to the fluctuating market conditions created by the high-level penetration of VRE.

The term 'flexibility' is currently used widely, and it is therefore important to establish definitions depending on the context and the timescales. A recent paper from Beiron et al. [9] has defined different types of flexibility, categorized according to plant-level (operational and product flexibility) and system-level flexibilities (thermal, electricity system, fuel supply and climate flexibilities). Operational flexibility is defined in that study [9] as the ability of a plant to vary its output by adjusting the input thermal load from the fuel conversion system. Among the different types of thermal power plants, solid-fuel boilers are the slowest in the operational flexibility spectrum (see [8][10]), especially those that burn low-grade fuels (to which renewable solid fuels typically pertain) such as biomass and waste. For the conversion of these fuels, fluidized bed combustors (FBCs) are the preferred technological choice due to the strong mixing and heat transfer capabilities offered. Thus, FBC plants play a crucial role in many energy systems around the world [11][12], and their operation is directly affected by the need for increased operational flexibility stated above. Yet, the vast majority of FBC plant setups are either: (i) larger coal-fired units for base-load electricity generation; or (ii) smaller biomass-fired or waste-fired units for combined heat and power (CHP) generation, with heat as the main output governing the plant dispatchability [11]. Moreover, the two existing types of FBC units, bubbling and circulating fluidized beds (BFB and CFB, respectively, with the latter having larger specific thermal capacity and typically larger sizes), have a large in-furnace solids inventory that yields plant systems that are characterized by delay, strong coupling among parameters and non-linear behaviors [13]. Thus, conventional operation of FBC units is characterized by small and slow load changes compared to other solid fuel combustion alternatives, such as pulverized coal plants [14], and the limits related to the transient capabilities of FBC units remain largely unexplored.

The importance of mastering the dynamic operation of FBC plants has been highlighted by several authors [15][16]. Investigations of the transient performances of effective control and

operational strategies would enable current FBC setups to increase their participation in various electricity markets, expand their product portfolio and, thus, remain financially attractive. Furthermore, large-scale FB reactors are at the core of several novel energy processes in early developmental phases in which the transient performance is foreseen as being crucial. Two major examples of these developments are: i) the retrofit of FBC plants into polygeneration facilities in which output energy vectors other than heat and power (e.g., fuel gas, char, hydrogen) are produced [17], [18]; and ii) thermochemical energy storage through solids cycling [19], [20], [21]. There are two main constraints that currently limit the introduction of flexibility into FBC plants in terms of load ramping. First, due to the complexity of the fluidization phenomena and the relatively large lack of industrial measurements, the inherent dynamics of FB boilers are still largely unknown, which means that fast ramping is a non-optimized process for most units, which may entail undesired consequences such as high emission levels [22]. Second, cyclic operation implies increasing stresses on plant components, and this results in reductions in equipment lifetimes and increased operational costs [23], [22].

Dynamic process modeling is gaining attention as a tool that can provide insights into the transient behaviors of power plants, as it allows operators and plant owners to evaluate various operational and control strategies that can lead to increased profits in the present and future energy markets [24], [25]. However, this strategy relies heavily on the reliability levels of the models used. While unit-specific models for conventional operation of existing furnaces and plants can be developed based on correlations derived from site measurements, general model formulations with a more solid theoretical ground are needed to study unit designs, sizes and operations outside the scope covered by site measurements. In particular for FB combustors, low-order, semiempirical models represent an optimal trade-off between accuracy, generic applicability, and low computational cost to be integrated into dynamic process models [26].

Alobaid et al. [25] have published an extensive review of dynamic modeling and simulation of thermal power plants, including a wide range of technologies and feedstocks, from which the following points can be extracted: i) there is a lack of dynamic modeling studies that focus on biomass-fired plants; and ii) there is very limited knowledge about the dynamic behaviors of FB boilers. Similar conclusions can be drawn from the recent review of Avagianos et al. [27], which is dedicated to dynamic modeling and simulation of solid-fuel power plants: there is a clear deficit of dynamic models that include FBCs, as well as of dynamic models of large-scale, biomass-fired units. Lastly, Atsonios et al. [15] have reviewed the existing dynamic process models of bio-based heat and power plants, highlighting the scarcity of such models as compared to models of fossil-fueled plants. Among the few published dynamic modeling investigations of biomass-fired power plants, the review highlights the scarcity of studies that account for the flue gas side of FB combustors, especially those that have been validated with site measurement data.

In summary, there is a growing need for FBC plants to increase their operational and product flexibility levels, in order to adapt to the new requirements associated with energy systems that have a high penetration of VRE. Due to the complexity of the fluidization phenomena, the lack of measurements from industrial-sized units, and the traditional steady operation of these plants, there is a knowledge gap regarding the transient capabilities of FBC plants. Although dynamic power plant modeling is a widely used tool to characterize and study the transient performance of power plants, very little work has been performed on the inherent and

controlled operational capabilities of FBC plants through thorough dynamic descriptions of both the gas and water-steam sides.

1.1.Aims and scope

The overall aim of this thesis is to characterize the dynamic behavior of large-scale FBC plants, so as to facilitate their transition into the forthcoming energy systems with high penetration levels of VRE. The scope of the work includes both the gas and the water-steam sides of commercial-scale FBC plants for combined heat and power production.

More specifically, this thesis attempts to fill the two major knowledge gaps by addressing the following research questions:

i) What are the inherent dynamics of FBC plants associated with load and fuel changes?
ii) How can control and operational strategies improve the operational flexibility of FBC plants?

To answer these questions, the present work makes use of semiempirical dynamic modeling to describe the transient performances of the reactor and water-steam process equipment of FBC plants. The specific objectives of the thesis are the following:

1) To develop a model that is capable of describing the dynamic behaviors of industrial-scale FBC plants while accounting for both the gas and water-steam sides.
2) To analyze the inherent dynamics of large-scale FBC plants when the load, fuel composition and district heating (DH) production level are varied.
3) To characterize the in-furnace mechanisms driving the inherent dynamics of FBCs.
4) To compare the dynamic behaviors of BFB and CFB combustors.
5) To evaluate the operational capabilities of FBC-CHP plants to provide fast load changes when operated under different control structures.
6) To assess the interplay between the dynamic responses of the gas and the water-steam sides.

1.2. Outline of the thesis

The present thesis comprises a summary dissertation and three appended papers. The dissertation consists of six chapters, for which the linkages with the three appended papers (**Papers I–III**) and the performed activities are depicted in Figure 1. After the introductory Chapter 1, Chapter 2 provides the background of the work and a literature review of the dynamic modeling assessments previously carried out for FBC plants. Chapter 3 presents the methods used in the work, Chapter 4 describes the formulation, calibration and validation of the dynamic models, Chapter 5 highlights and discusses the main findings of the work, and Chapter 6 concludes the thesis in relation to the aims, research questions and objectives set, and incorporates a brief discussion on future work.

As shown in Figure 1, the model of the gas side is capable of describing both BFB and CFB combustors; and an FBC-CHP plant model has been developed from integrating the gas side model into a dynamic process model of the water-steam side. Operational data from two reference units are used for the calibration and validation of the dynamic models. Lastly, the furnace and plant models are used for carrying out various dynamic analyses of the gas and water-steam sides of CFB and BFB units, including examinations of control and operational strategies imported from the literature. The findings of this thesis are of relevance to various thermochemical processes where large-scale FB reactors are expected to operate dynamically, as further discussed in Chapter 6.

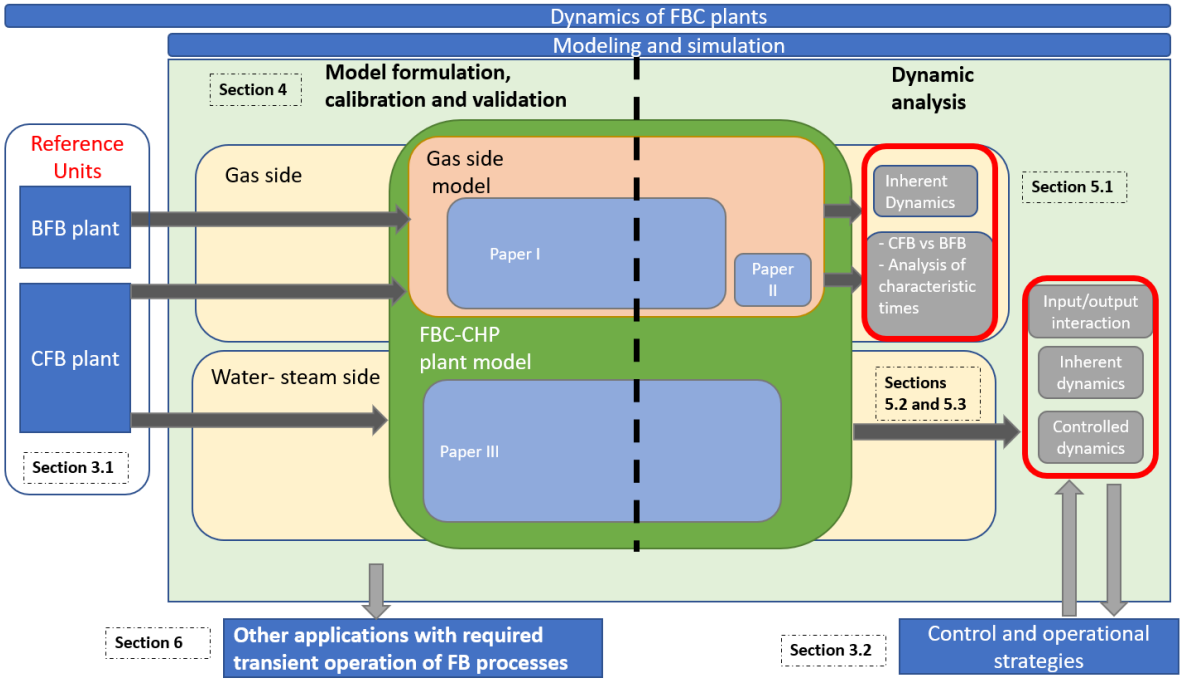

Figure 1. Schematic of the thesis structure. Light green area: Modeling and simulation activities. Dark blue boxes: non-modeling activities. Yellow boxes: scope within FBC plants. Grey boxes: outputs from the analyses. Light blue: appended papers.

Paper I presents a dynamic model of the gas side of large-scale FBC plants. The model, which is capable of describing both BFB and CFB furnaces, is validated against operational data from one reference unit of each type. After the formulation, calibration and validation of the model, the paper focuses on studying the partial load performances of the reference units prior to the analysis of the inherent dynamic behavior of the gas side when the load and fuel composition are changed.

Paper II uses the gas side model presented in **Paper I** to compare the transient performances of BFB and CFB furnaces after eliminating the thermal size effects (given that two units of the same size, 130 MW_{th}, are simulated). Furthermore, the paper investigates the impacts of the characteristic times for each of the dominant in-furnace mechanisms (fluid dynamics, fuel conversion, heat transfer) on the stabilization times of the furnace temperatures and heat extraction in BFBs and CFBs.

Paper III investigates the transient capabilities of CFB-CHP plants, including both the gas and the water/steam sides. The gas-side model presented in **Paper I** is integrated into a dynamic

process model of the water-steam side, and the resulting integrated FBC plant model is validated against steady-state and transient operational process data obtained from an industrial CFB-CHP plant. The paper includes a comprehensive review of the main control strategies for load changes applicable to CFB-CHP plants. Finally, the paper studies the interactions between the inputs (e.g., fuel and air flows) and outputs (e.g., power and heat production) of the plant, the inherent dynamics of the process at the plant level, and the performances of the different control and operational strategies in providing fast load changes.

2. Background and related work

2.1. Power plant flexibility

It is known that operational flexibility is needed to handle variations in plant load over a wide range of magnitudes and time scales. The timescales range from seasonal, caused by changes in air temperature or fuel composition, to hourly, required to match the needs of societal daily patterns as well as day-ahead market operations, and even down to shorter timescales (minutes and seconds), required for voltage and frequency control. Operational flexibility includes the following key aspects [28]:

- High cycling capability: increasing the speed of load ramping and start/stop of the plant allows the plant to provide grid stabilization services, although this requires advanced process control (in addition to plant components of good quality that can withstand the increased thermal stresses).
- Part-load efficiency: As the share of VRE increases in a certain power market, it is expected that thermal power plants will operate at off-design (i.e., partial) loads for long periods of time. Thus, plant efficiency at partial loads becomes crucial from both the economic and environmental perspectives.
- Expansion of the operational boundaries: Overload capability (i.e., production at 105%–110% load) allows the plant to deliver excess output at times when additional production is beneficial. In contrast, reducing the minimum load offers the possibility to reduce the production level during those periods when it is not economically attractive to produce power or when reducing the load generates revenue, while avoiding the costs associated with stop/start of the plant.

Apart from operational flexibility, product flexibility attains importance in plants that produce more than one output, i.e., CHP or polygeneration plants, by decoupling the production of the outputs, as it enables the possibility to prioritize the generation of a specific product based on market conditions. In the case of CHP plants, this can be achieved, for instance, by partial or full turbine bypass [29], [30] or hot water accumulators [31], among other means [32],[33]. Furthermore, decoupling the production of heat and power allows CHP plants to participate in electricity-driven markets rather than being concerned with dispatch based on heat demand only [34].

In solid-fuel power plants, the variations in fuel properties (e.g., moisture content, heating value) represent critical sources of variations that require power plant flexibility [27]. The plant is required to respond to disturbances in fuel properties on seasonal, daily and batch bases, especially when dealing with low-grade fuels such as biomass or waste. Moreover, FBC units are often used for the co-firing of coal and renewable solid fractions, which creates an additional source of variations related to varying the fuel mix [35].

Within a thermal power plant, the control system is responsible for the regulation and coordination of all the involved subsystems, so as to fulfil a certain operational objective while ensuring safe operation [36],[37]. Currently, the control solutions deployed in industry are often based on traditional practices and are not necessarily optimized for fast load changing or

maximal plant efficiency. However, as the need for operational flexibility increases, the effective design, tuning and deployment of advanced control strategies gain relevance as tools to increase the operational and production efficiencies of the plant, thereby avoiding expensive retrofits [38].

2.2. Fluidized bed combustion

A gas-solids fluidized bed consists of a vessel in which a bed of bulk solid particles adopts a fluid-like behavior when a gas is injected from the bottom of the vessel. Fluidized beds are known to exhibit high mass and heat transfer capabilities due to the relatively high mixing rates of both the solid phase and gas phase [39]. Furthermore, the thermal capacity associated with the large mass of bulk solids yields relatively homogeneous furnace temperatures, which are advantageous in terms of efficiency and emissions, especially in the case of thermochemical conversion of low-grade solid fuels [11]. In addition, FBCs enable the in-bed capture of CO_2 through the use of sorbents as bed material, as well as the efficient handling of different fuel types and even mixtures thereof [35].

Fluidized beds can generally be divided into the dense bed, which is located at the bottom of the reactor and characterized by a large concentration of solids, and the freeboard, which is located immediately above the dense bed. In this freeboard, a splash zone characterized by a strong drop in solids concentration with height is established after solids ejection from bubbles that are erupting at the dense bed surface and solids backmixing to the dense bed. While this summarizes the picture for BFB units (Figure 2a), in CFB units a combination of higher gas velocities and finer solids yields entrainment of solids above the splash zone (in the so-called transport zone) and the establishment of a significant solids flow also at the upper furnace locations (see Figure 2b). This disperse solids flow backmixes gradually by separation at the furnace walls and, eventually, a minor share of the solids is recirculated externally to the furnace after being separated from the gas in a cyclone. In FB boilers, heat is typically extracted from the furnace through membrane tube walls, as well as from the convective flue gas path, where economizers and superheaters are located (also included in Figure 2). It is common that in CFB units, which typically have larger thermal capacities and sizes, there are additional heat transfer surfaces in the furnace, cyclone and/or loop seal, in order to close the heat balance with a furnace temperature of around 850°C.

At present, FBC units are used to produce power, heat, and a combination of these. When deployed for power production only, large (with sizes up to 500 MW_{el}) coal-fired CFB units are the preferred option, owing to the higher energy density of coal and the superior heat transfer capabilities of CFB units. Alternatively, FBC units deployed for the production of heat for a nearby DH system or industrial process are often of smaller size (typically $\leq$ 100 MW_{th}) and make use of low-grade fuels such as biomass, waste and other waste-derived fuels. Due to the large demand for heat in regions with large volumes of biomass, such as Sweden, the production of heat is the main economic incentive of FBC plants, although the production of electricity often represents a side-revenue for the process.

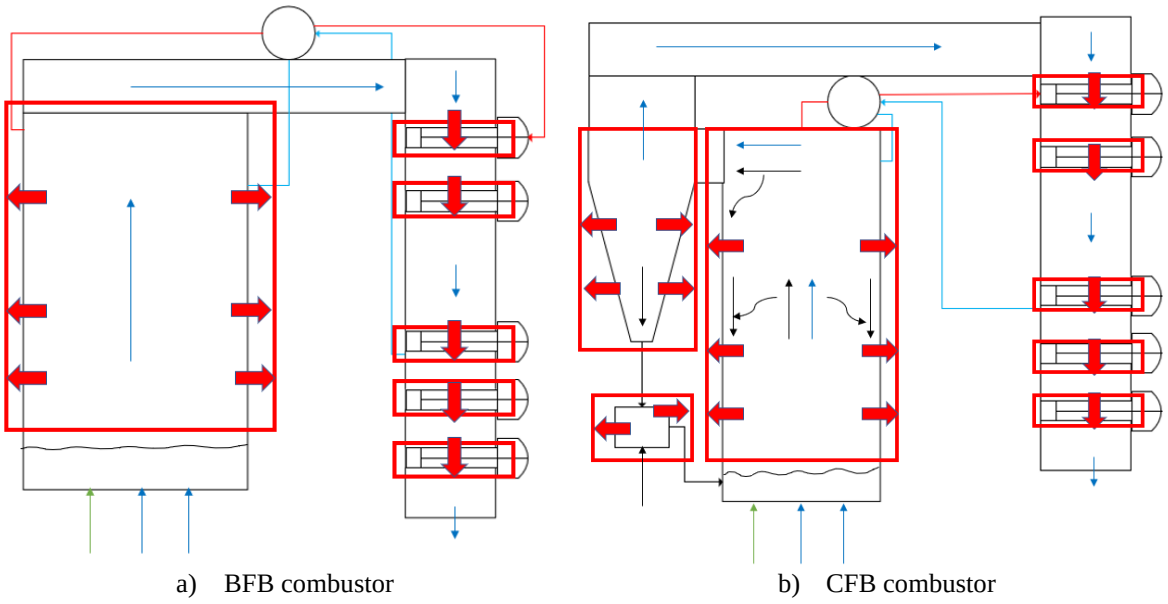

Figure 2. Schematic of the two main types of FBCs. Arrows show the main heat transfer from the gas side to the water-steam side.

2.2. Dynamic modeling of FB boilers

Mathematical modeling of power plants represents an essential tool for plant design, operation and optimization, as it allows the investigation and understanding of the process behavior, capabilities and limitations. Furthermore, dynamic modeling can be used to assess the flexibility of a specific existing or future process and to test control and operational strategies, as well as, for instance, to train plant operators. Over the last decade, extensive research studies have been published regarding the dynamic modeling of power cycles, such as Rankine cycles for coal-fired power plants [40],[41], combined-cycle plants [42], [43], waste-fired units [44], [45], nuclear plants [46], and concentrated solar power [47]. Nevertheless, one of the aspects that most of these works share is the assumption that the gas side of the boiler has a much faster response to operational variations than does the water-steam side, and so its dynamics can be neglected. Although the validity of this assumption has been proven for gas-fired combustion [48], [49], it has not been explored for FBC plants.

When it comes to modeling the dynamics of the gas side of FB boilers, most of the available literature has focused on CFB units. Several 0D models [50], [51], [52] have been presented and used in the literature, although they are not capable of describing the special distribution of the solids throughout the furnace, which is a crucial aspect of CFB operation. One of the first 1D dynamic models published was that of Park and Basu [53]: a mathematical representation of a 0.3-MW furnace that was capable of predicting the transients of char and oxygen concentrations. A 1D model was presented by Majanne and Köykkä [54], in which an evaporator model was linked to the gas side, allowing simulations of the steam pressure and mass flow after a change in fuel moisture, with stabilization times of the water/steam side in the order of 10 minutes. Recently, Deng et al. [55] have modeled the 1D dynamic behavior of the solids flow of a 350-MW unit, observing abrupt transients when increasing the gas

velocity. More detailed models include the internal recirculation of solids through the wall layer. The 1D models that include this feature are typically called 1.5D models. Among these, the model presented by Chen et al. [56] of a 410 t/h coal-fired unit stands out as having being validated with operational data from an industrial site. After presenting and validating the model, the work focused on the qualitative analysis of the trajectories of the main in-furnace variables after a load change. More recently, Kim et al [57] have presented a 1.5D model of the gas side of CFB units that was validated with design data from a coal-fired 795-MW plant. The model was then applied to investigate the effect of the solids flow on the transient responses of the CFB loop, revealing overshoots in the temperature responses for certain load changes. A 1.5D dynamic model presented by Ritvanen et al. [58] and based on a previous publication [59] has been widely used for simulation and control studies [60], [61], [62]. Haus et al. [63] have presented a dynamic model of the gas side of interconnected FB reactors with the focus on chemical looping combustion. That model was successfully validated against tests conducted in an experimental facility. Lastly, it is important to mention that some other groups have developed dynamic models of the gas side as a way to design and test control strategies (see for instance [64]), where the high level of interaction between variables was highlighted.

Regarding the gas side of BFB units, Kataja et al. [65] have presented a 1D model connected to a model of the steam drum and evaporator, and used this to simulate the boiler responses after a step-change in fuel flow. A detailed model has been described by Selcuk [66], presenting a validation of the model with steady-state and transient data obtained from a 0.3-MW unit. This model was subsequently used to investigate the dynamics of the unit, identifying inverse responses in the char inventory of the dense bed after a load increase. A model of a biomass-fired BFB combustor has been developed and used by Galgano et al. [67], who uncovered large differences in the dynamics of the dense bed and in the freeboard caused by the differences in heat capacity between the different regions.

Other studies have investigated the transient behaviors of FBC plants by focusing on the dynamics of the water-steam side, especially in coal-fired CFB units. Hultgren et al. [68] made use of the CFB model presented previously [59] to perform a control design analysis of a coal-fired CFB plant, identifying large interactions between the control loops, i.e. manipulation of one input affected several outputs. Their work was further expanded upon [69] to create an integrated control process design (ICPD) to optimize the transient performance of the steam side, resulting in very good load-tracking performance under boiler-following operation. Nevertheless, the authors stated the need for a detailed mechanistic model to improve the robustness of the study. Gao et al. [13] have presented and validated a 0D model of a CFB furnace that accounts for the water-steam side tubes. Following linearization, this model was used by Zhang et al. [14] for model predictive control (MPC). The 1.5D model of the gas side presented in [57] was integrated into a model of the water-steam side by [70] and utilized to quantify the responses of the steam temperature after changes in the fuel and feedwater flows. Recently, Stefanitsis et al. [61] have used the CFB model originally published in [59] to evaluate the transient performance of a boiler after implementing a thermal storage in the form of hot bulk solids, and they concluded that the stabilization time for load changes is reduced when adding the storage. In recent times, some authors have investigated the transient behaviors of waste-fueled CFB plants. Zimmerman et al. [71] have exploited a 0D model of the gas side presented earlier [50] to compare different control strategies, identifying feed-forward (FF) MPC as the optimal strategy in terms of disturbance rejection. Beiron et al. [45]

have presented and validated a detailed dynamic model of the water-steam side of a waste-fired CFB unit, and have further applied the model to investigate the inherent dynamics of the process. Regarding BFB plants, it is worth mentioning the recent work of Zlatkovij et al. [51], in which a 0D dynamic model of a BFB furnace integrated into a simplified model of the water side was used to test and compare MPC strategies, highlighting FF-MPC as the preferred option.

The literature review presented in this chapter in combination with more dedicated literature reviews in **Papers I** and **III** justify the aim of this thesis as presented in Section 1.1, as there is a clear lack of:

i) assessments of the dynamics of FBC plants that include a description of the dynamics of both sides, i.e., the gas and the water-steam sides.

ii) studies focusing on the transient performances of biomass-based units of smaller size for the production of CHP; and

iii) models that are validated against steady-state and transient operational data obtained from large-scale FBC plants.

iv) Assessment of control structures for FBC-CHP plants in a systematic way.

3. Methods

This chapter gives an overview of the main methods used in the thesis. First, Section 3.1 describes the large-scale FBC furnaces and plants used as references in this work, i.e., those from which operational data were collected for model calibration and validation (**Papers I** and **III,** Chapter 4) and in which the dynamics were studied. Thereafter, Section 3.2 briefly discusses the procedures for modeling formulation and simulation, while Section 3.3 presents the different procedures for the dynamic analyses carried out throughout the work (**Papers I**–**III**).

3.1.Reference units

3.1.1. BFB and CFB furnaces

Two industrial furnaces with sizes, designs and operational conditions representative of biomass-based FB boilers were selected as references. A simplified pipping and instrumentation diagram (P&ID) of each of the units, including the instruments selected for data collection (see Section 3.1.2), is shown in Figure 3, and the nominal compositions of the biomass (wood chips) regularly used as fuel in each of the units are listed in Table 1.

The reference 100-MW_{th} CFB unit (Figure 3a) has a furnace with dimensions of 8.5×4.1×21 m^3 which is coupled to two parallel cyclones with corresponding diplegs. The fuel-feeding ports are located in the return pipes. The furnace has secondary air injection ports located between 1.5 m and 3 m above the bottom gas distributor. Above the refractory-lined region (up to a height of 4.5 m), the furnace is composed of membrane-type waterwalls. The furnace has a tube-bundle superheater in the riser at a height of 11 m.

The reference BFB furnace (Figure 3b) is a 130-MW_{th} with dimensions of 9.18×8.67×30 m^3 and operated with a dense bed height of approximately 0.5 m. Secondary and tertiary air streams are injected at heights of 2.5 m to 10 m, respectively, above the nozzle level. Part of the cold flue gas can be recirculated for bed temperature control. The furnace walls and roof consist of membrane waterwalls located above the refractory-lined bottom section (up to a height of 2.5 m). Two superheaters in the form of three tube bundles in total are immersed in the upper part of the furnace.

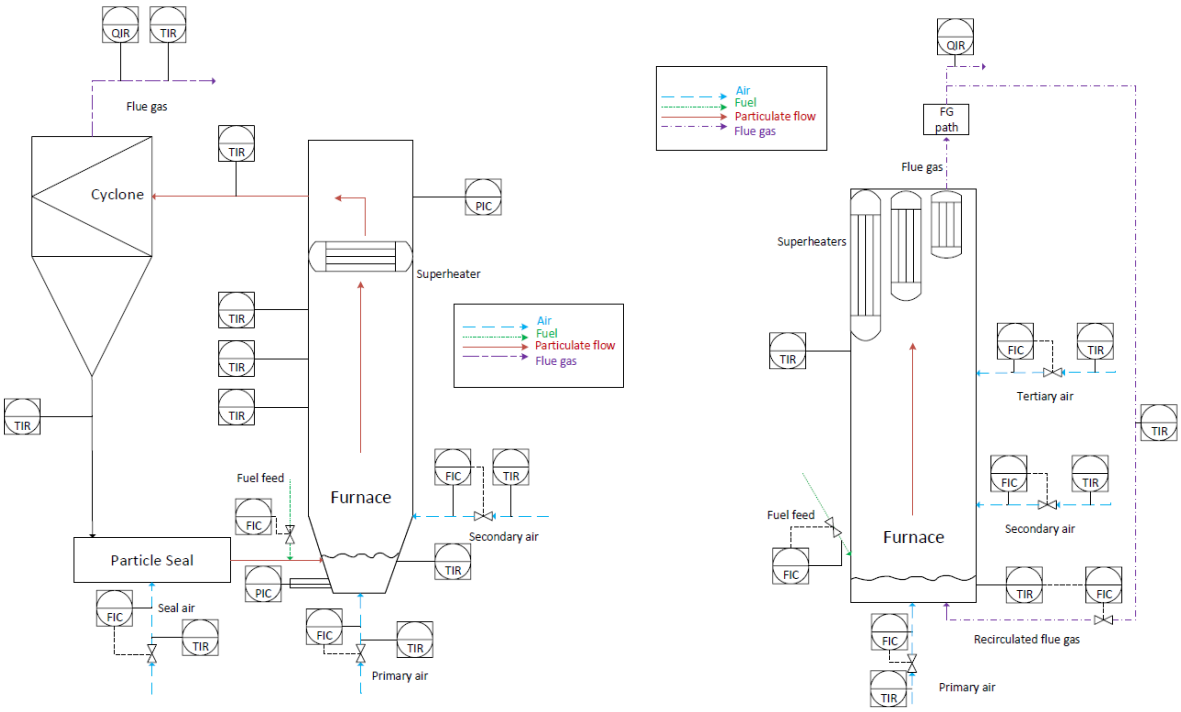

a) CFB unit b) BFB unit

Figure 3. Schematic piping and instrumentation diagram of the reference units. Source: **Paper I**

Table 1. Proximate and ultimate analyses and heating values of the reference biomass used in the reference plants. **Source: Paper I**

Proximate Analysis wt%	**CFB furnace**	**BFB furnace**
Moisture	54.00	40.00
Volatiles	32.00	47.00
Char	13.60	12.60
Ash	0.40	0.40
Ultimate Analysis wt% (dry ash-free)		
C	50.60	
H	5.90	
O	43.20	
N	0.08	
S	0.04	
HHV (dry, ash-free), MJ/kg	17.0–18.5	17.9

3.1.2 CFB-CHP plant

The reference CFB unit generates superheated steam for the production of DH and electricity. The boiler is one of the three units that compose the DH system of the City of Karlstad in Sweden [72], and it is operated as a mid-merit type, i.e. adjusting its output for daily changes in heat demand. The plant is a subcritical, single-pressure steam cycle, which is typical of CHP plants in Sweden. A simplified process diagram of the plant is shown in Figure 4, indicating the main regulatory and supervisory control loops, as well as the names of the different process equipment. The feedwater line flowing into the drum is first preheated in the economizer. From the drum, the saturated water-steam mixture naturally circulates through the evaporator tubes

located in the furnace waterwalls. The generated steam is then superheated before expanding in the steam turbine. DH water is produced in the last turbine condenser, whereas two additional steam extractions are used for feedwater preheating. Note that according to this process arrangement, the production of heat and power are linked through a constant power-to-heat ratio (of around 0.36 in this specific case).

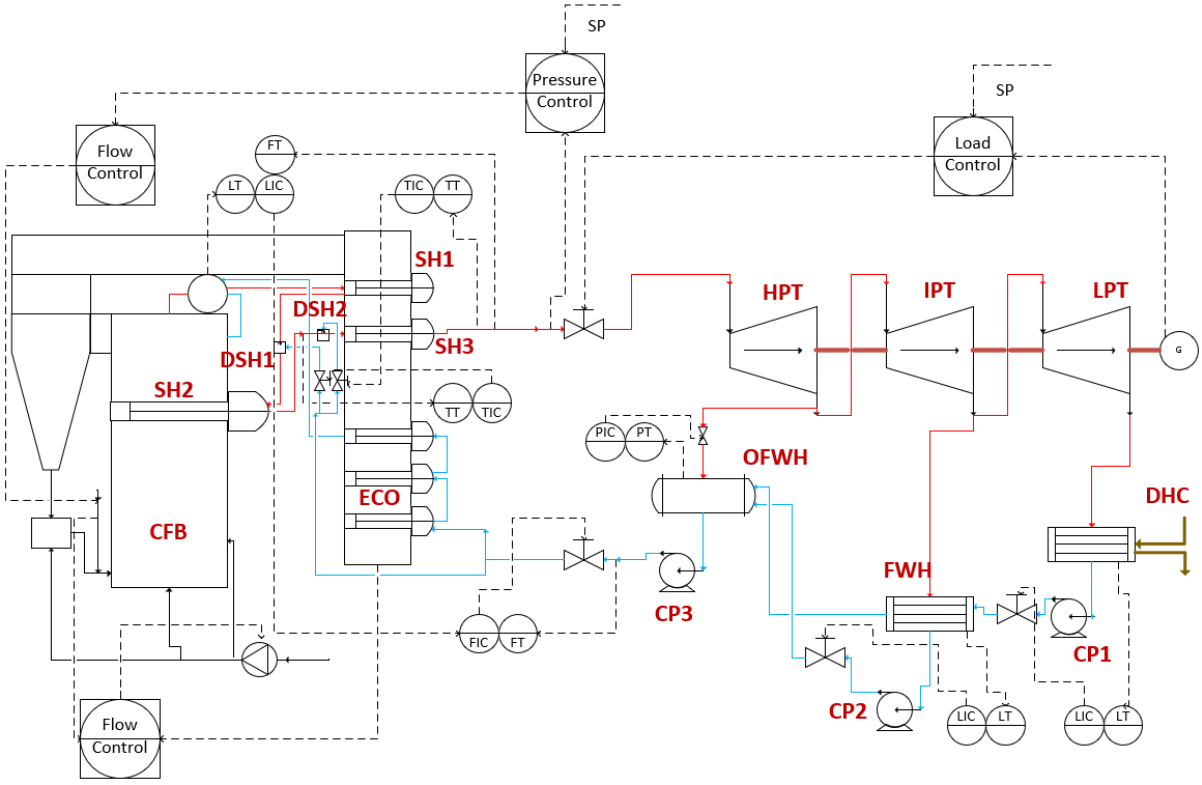

Figure 4. Schematic diagram of the CFB-CHP reference plant. Name tags of the main process equipment: SH: superheater. DSH: desuperheater. ECO: economizer, HPT: high pressure turbine. IPT: intermedium pressure turbine. LPT: low pressure turbine. OFWH: open feedwater heater. FWH: feedwater heater. DHC: district heating condenser. CP: centrifugal pump. Supervisory and control structures are shown: L: level. F: flow, T: temperature. Source: **Paper III**

3.1.2. *Data acquisition*

The reference units presented above were used to collect both operational plant data and design information of the main process components. Following a systematic approach for the data collection and analysis is required when dealing with complex plants as the ones of this work. Thus, the following steps summarize the data acquisition process followed for collecting and processing the datasets used in this work:

- Step 1 - Instrument and data selection: Studying the P&IDs containing the flows, vessels, controllers, and instruments present in each of the units conforming the plants is a mandatory first step in the data acquisition process. Subsequently, the instruments of interest, i.e. the measurements and set points containing variables of interest for the model development are selected and requested. Variables of interest include temperatures, pressures, flows, levels and concentrations. In parallel to the instrument selection, geometric design data of the modeled equipment were selected, such as dimensions, pitch and number of tubes, existence of fins or metal thicknesses.

- Step 2 - Time period selection: For the steady-state calibration and validation of the model, different operational periods at which the plants were running at diverse load levels were requested. Steady-state datasets involved periods of 1-2 hours of operation. Regarding transient operation, periods in which the load was increased and decreased were requested. The transient datasets used in this work are periods of 3h of operation. The resolution of both steady-state and transient datasets was the minimum that the plant instruments could provide, i.e. 60 seconds.
- Step 3 - Post-processing data: Steady-state data used in this work was calculated as the average of 30-minute measurements (see **Paper I** for details). For the transient validation (see Section 4.3.3), the measured transient datasets were linearly interpolated from the sampling time scale of 1 min into a time scale of 1 second.

3.2. Modeling and simulation

Dynamic models of thermal power plants are those capable of describing both the steady-state behavior at several load levels (i.e. design and off-design behaviors) as well as the transient behavior of the process when the operating conditions are changed, capturing the timescales and physical phenomena of the changes of interest. In this work, dynamic models of the gas and water-steam side of FBC plants are developed using Modelica [73]. The model also includes regulation components such as controllers, ramps, steps and other mathematical blocks. The formulated dynamic models result in a differential-algebraic system of equations (DAE) solved by means of the numerical solver Radau IIA [74]. In order to capture the fast-transient events typical of combustion processes, the selected time resolution for the dynamic analysis was 1 second. This was increased to 100 seconds for steady-state analyses. Initialization of the model was done by assigning design values to the main state variables.

To simulate the reference units, the models are first parametrized with design plant data and after that calibrated and validated with steady-state and transient operational plant data from the reference units described in Section 3.1. The calibration and validation of the gas-side model with data from the BFB and CFB furnaces are described in **Paper I**, while the validation and calibration of the CFB-CHP model accounting for both the gas and water-steam sides are presented in **Paper III**. Figure 5 summarizes the operational datasets used for calibration (green boxes) and validation (grey boxes), respectively. As indicated, for the reference CFB unit the model (encompassing the gas and water-steam sides) is calibrated to match the steady-

state operational dataset at 100% load. For the BFB reference furnace, the model is calibrated with steady-state data at 100% and 40% load.

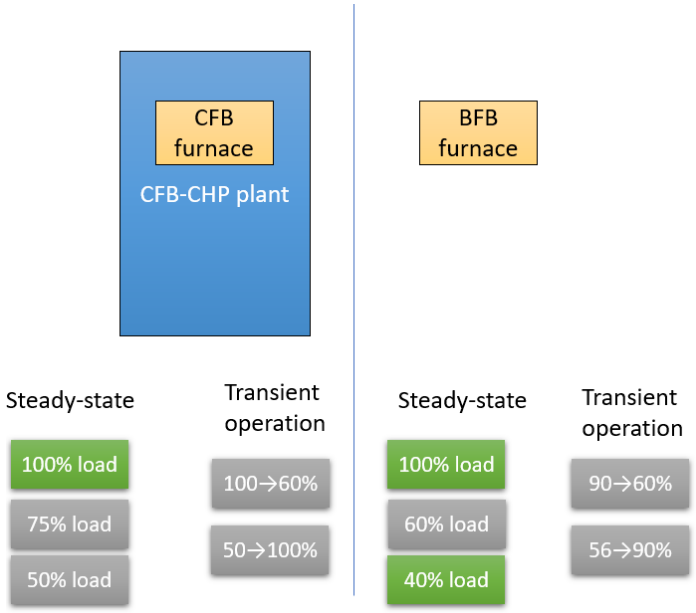

Figure 5. Operational datasets acquired from the reference plants and used for model calibration (green boxes) and validation (grey boxes). Yellow boxes refer to the gas side model and blue boxes to the integrated plant model.

3.3. Dynamic analyses

This section describes the methods employed in the dynamic analyses for the evaluation of the inherent and controlled transient performances of FBC plants through dynamic simulations.

3.3.1. *Inherent dynamics*

The inherent dynamics of a certain system are commonly evaluated through open-loop tests. These tests involve the introduction of individual step-changes in the key process inputs when the system is uncontrolled, after which the trajectories of the variables of interest are tracked. Thus, an open-loop analysis enables an assessment of how the system responds to the effect of a specific change while minimizing/cancelling the impact of the control layer. Performing this type of tests in industrial plants is often not possible due to safety and operational constraints as well as due to the presence of non-optimal control loops, what makes mechanistic dynamic models a great alternative for the investigation of the process inherent dynamics.

Table 2 lists the changes studied through open-loop tests in each of the appended papers, specifying the step magnitudes and the loads at which the boilers were running when the steps were introduced. Process variables typically important for operation are used to characterize the transient performances of the gas and water-steam sides, included in Table 3. The responses of these variables are assessed in terms of the total stabilization time [t_s, see Eq. (1)], which is defined as the time it takes for a certain process variable y to remain within an error band of ±10% of the total change in steady-state values. The relative change (RC) of the process

variables between their initial and final steady-state values is also computed according to Eq. (2). Figure 6 includes a simplified representation of how t_s and RC are computed.

Table 2. Step changes (magnitude and variable) input in the model for the open-loop tests.

	Input variable changed	Simulated steps
Paper I	Combustion load, Q_{comb}	-15%, ±25% and -50% at 100% load
	Fuel moisture content, $\%_{H2O}$	±5% at 100% load and at 75% load
Paper II	Combustion load, Q_{comb}	-15% at 100% load
	Fuel moisture content, $\%_{H2O}$	+5% at 100% load
Paper III	Combustion load, Q_{comb}	±20% at 70% load and at 80% load
	Fuel heating value, HV_f	±20% at 70% load and at 80% load
	DH water flow, F_{DH}	±20% at 70% load and at 80% load
	DH water inlet temperature, $T_{DH,in}$	±20% at 70% load and at 80% load

Table 3. Process variables tracked to characterize the inherent dynamics

Gas side
Temperature of the dense bed, T_{db} [˚C]
Temperature at the top of the furnace, T_{top} [˚C]
Total heat transferred to the waterwalls, Q_{walls} [MW]
Water-steam side
Power produced, P_{el}, [MW]
DH load, Q_{DH}, [MW]
DH water outlet temperature, $T_{DH,out}$ [˚C]
Live steam mass flow, F_{steam} [kg/s]
Live steam pressure, P_{steam} [bar]

$$t_s = \tau\rfloor_{y_0 \rightarrow y_\infty \mp 0.1(y_0 - y_\infty)} \quad (1)$$

$$RC = 100 \cdot \frac{y_\infty - y_0}{y_0} \quad (2)$$

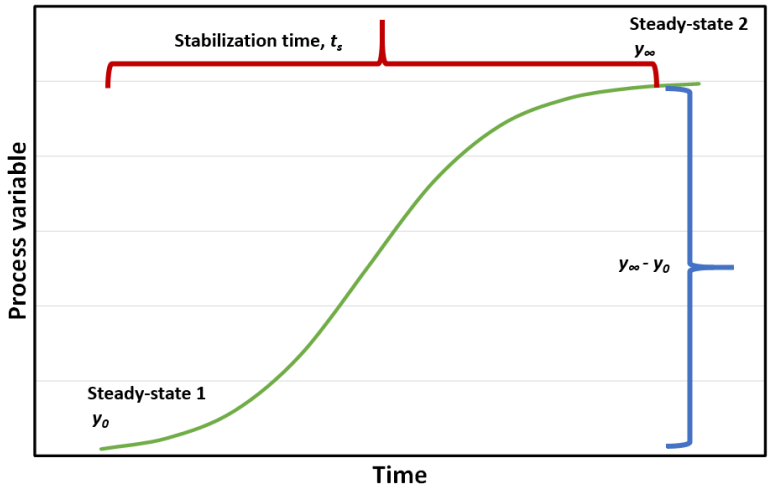

Figure 6. Schematic of how stabilization time and relative change are computed from the transient trajectory of a certain process variable

Paper II carries out a comprehensive comparison of the transient performances of the gas sides of BFB and CFB furnaces of the same size. For this, the stabilization times of the different

variables listed in Table 3 are studied through open-loop tests as a function of the characteristic times of the main gas-side mechanisms (i.e., fluid dynamics, heat transfer and fuel conversion; see Chapter 4).

3.3.2. *Controlled dynamics*

The supervisory control layer of a process plant is responsible for regulating the variables of importance from the production point of view, i.e., driving the plant economics in a longer timeframe [38]. In thermal power plants, the supervisory control structure works on a minute-hour timescale, handling variations in the fuel composition and load. In particular in steam-generating plants, such as those investigated in this work, the supervisory control system modulates the steam flow, temperature, and pressure, so as to target production values. Complementary to this, the regulatory control layer takes care of stabilizing the process so that it does not drift away from acceptable operating conditions during disturbances. This translates into the control of vessel pressures, levels, and in some cases, temperatures.

Supervisory control strategies for boilers differ in with respect to whether the power plant output (i.e., generated power and heat) is controlled by the combustion load (i.e., air and fuel flows into the furnace) or by the live steam control valve. The operational implications of each of the most-common standard boiler control strategies used to provide fast load changes in FBC plants are briefly described below, schematically shown in Figure 7 and reviewed in **Paper III**.

- Boiler-following operation (BF): The master load controller manipulates the live steam control valve, which yields a change in the live steam pressure that is corrected by the pressure controller that manipulates the combustion load.
- Turbine-following operation (TF): The master controller uses the combustion load to control the load, while the live steam pressure is controlled by the opening of the steam control valve.
- Floating pressure operation (FP): In this operational strategy, the live steam pressure is not controlled, and instead fluctuates with boiler load as a result of the energy balance in the boiler. Thus, the load is controlled with the combustion load and the live steam control valve remains open.
- Sliding pressure: As a variant of FP operation, the pressure is controlled but not fixed. The set-point of the live steam pressure is a function of the boiler load (and is commonly measured using the live steam mass flow) and it is controlled by the combustion load. Thus, the plant load is controlled by the steam control valve opening.
- Hybrid control operation: As an enhanced version of the sliding pressure method, this strategy combines constant pressure operation at high boiler loads with variable pressure at lower loads (see [75] and [76]).

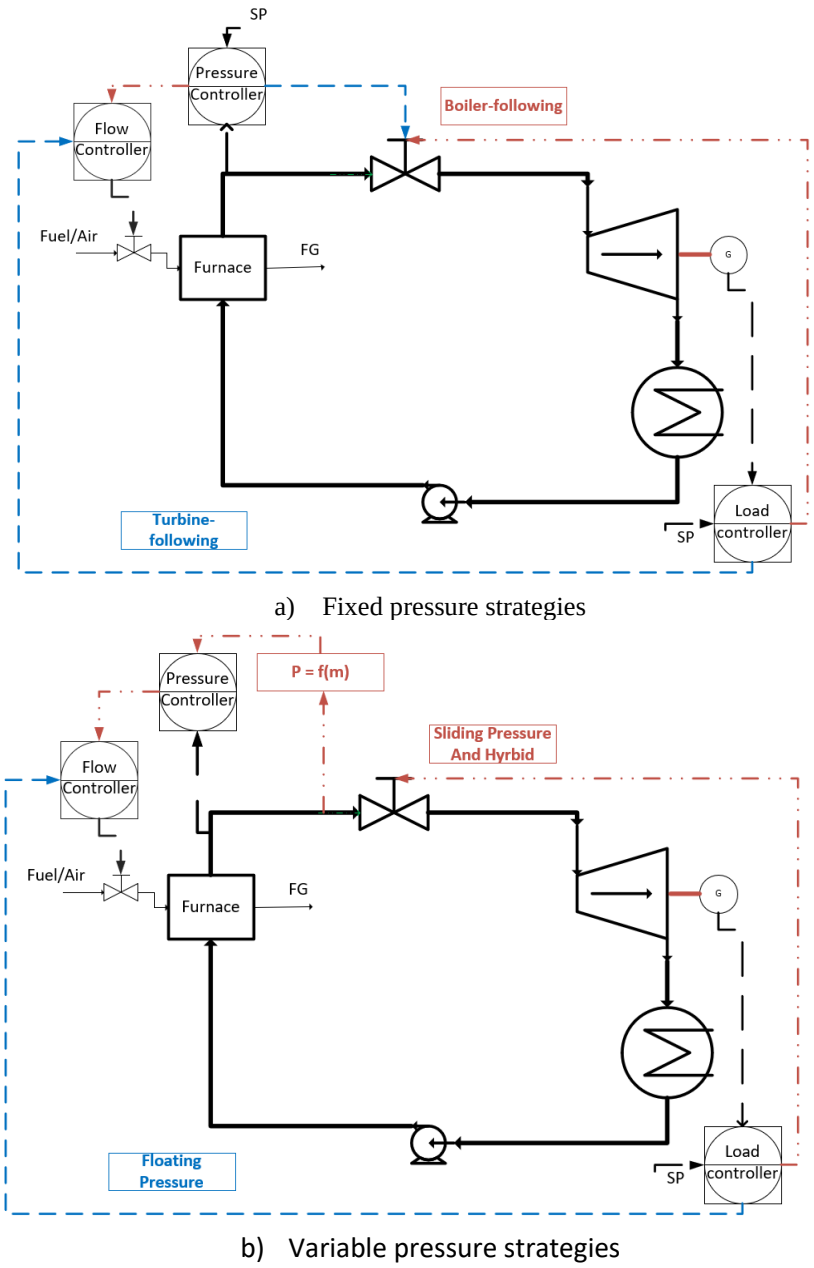

Figure 7. Supervisory control strategies for load changes. Source: **Paper III**

Variable ramping rate analysis

In order to assess the performances of FBC plants at rates that are typical for industrial operation, load changes at different ramping rates are investigated. While **Paper I** evaluates the implications of load ramping speed on the in-furnace dynamics, **Paper III** evaluates the load changing performance of the CFB-CHP plant when operated under different control strategies and for several ramping rates (see Table 4). The rise time of the generated power, i.e., the time that it takes for the output power to go through the 10%–90% response window [77], is used in **Paper III** to assess the performance of each control strategy.

Table 4. Magnitude and rate of the load changes simulated in the variable ramping rate (VRR) analysis

	Load change	Ramping rate
Paper I	100%→75%	-0.41%/s -0.041%/s
Paper III	100%→50%	-0.005%/s -0.05%/s -0.5%/s -5%/s
	50%→40%	-0.001%/s -0.01%/s -0.1%/s -1%/s

4. Dynamic model

A dynamic model of large-scale FBC plants is developed in this work, and it is used for generating the dynamic responses, which are analyzed as described in Chapter 3 (see **Papers I–III**). This chapter describes the formulation, calibration and validation of the overall dynamic model, resulting from integrating two dynamic models: one describing the gas side of FBC plants (described in detail in **Paper I**), and one describing the water-steam side (presented in **Paper III**). External inputs required for the integrated model are:

- Boiler and equipment geometry, including location of fuel and air feeding injections.
- Bulk solids properties: namely the density and size of the in-furnace bulk solids.
- Riser pressure drop, i.e.
- Fuel and gas composition and properties, including feeding temperatures.
- DH inlet conditions: flow, temperature and pressure of the return DH entering the plant.
- Operational conditions dictating the operation of the reference plant, i.e. set points for load level, live steam temperature and/or pressure, etc.

Figure 8 shows a schematic of the input/output flow diagram of the two integrated models, including the master control governing the plant operation and the internal model variables through which both sides are connected. The following aspects of the model integration in the present work are particularly noteworthy:

- The flue gas stream leaving the gas side enters the water-steam side model *via* the convection path.
- The furnace waterwalls transfer heat from the gas side for evaporating the biphasic water-steam flow, which in combination with the thermal inertia of the wall material determines the dynamics of the wall temperature. This heat transfer through the walls and wall temperatures are represented in Figure 8 by a single arrow for simplification. However, these are handled in the model as control volumes in each of which a dynamic energy balance is solved (see Section 4.1 for details).
- The superheaters that are immersed in the furnace at height h extract heat from the corresponding control volumes of the gas side while simultaneously superheating steam in the water-steam side.

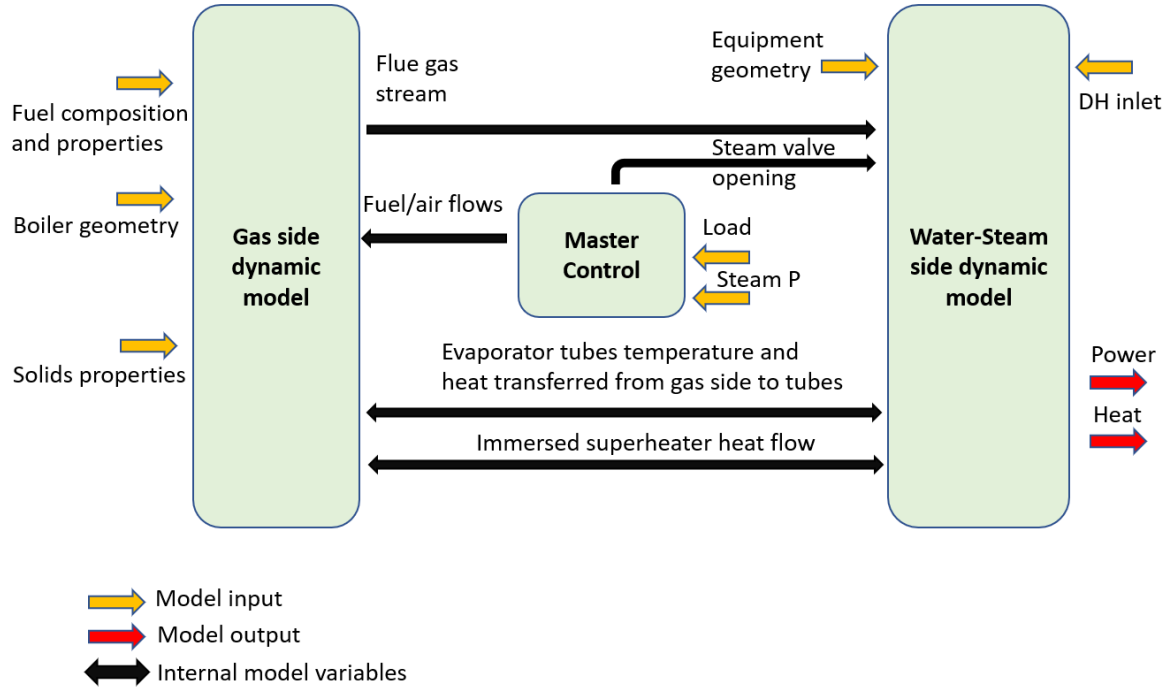

Figure 8. Input/output scheme of the integrated dynamic model including the master control. Source: **Paper III**

4.1. Gas side

The gas side (see glossary and Figure 9 for the definition and boundaries, respectively) is described by a number of perfectly mixed control volumes (CSTR) that exchange mass and energy (Figure 10). The domain is divided into the different fluid-dynamic regions that are generally identified from experimental studies in large-scale FBCs [78], [79], [80]: the dense bed and freeboard, and for CFB boilers, also the exit zone, cyclone and loop seal. The regions that are known to exhibit a plug-flow behavior, and thus deviate from the assumption of perfect mixing (such as the gas in the dense bed or gas and solids in the freeboard), are described in terms of a consecution of CSTRs. The model accounts for three phases consisting of the: gas (comprising an ideal gas mixture of nine phase components); fuel (modeled as three phase components – fresh, dry devolatilized, and char – to account for the changes in size and density that occur during conversion); and bulk solids (represented by a mean size). The model solves the intercoupled dynamic energy and mass balances for each of the control volumes, computing the temperatures and heat flows, as well as the concentrations and mass flows of each of the phase components. These energy and mass balances are governed by three main mechanisms defined below and briefly described in the following subsections:

- Fluid dynamics: description of the gas and solids flows within the furnace.
- Fuel conversion: drying, devolatilization and homogeneous and heterogeneous combustion of the fuel.
- Heat transfer: Transport of thermal energy within the furnace and from/to the waterwalls.

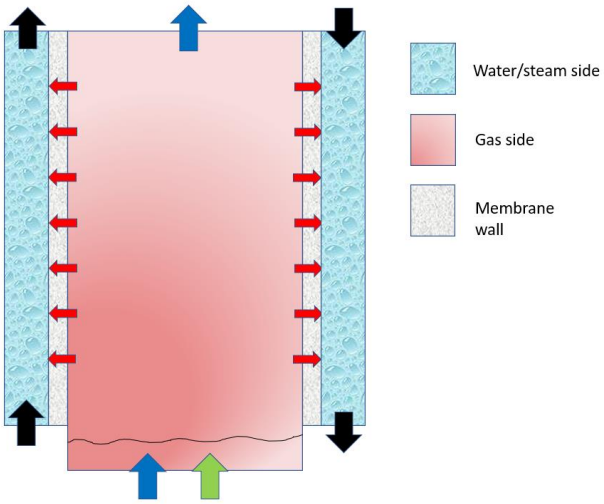

Figure 9. Schematic of the general layout and boundaries of gas side, water-steam side and membrane wall. Green arrow is fuel, blue arrows are gas, black arrows are water-steam flows and red arrows are heat flows

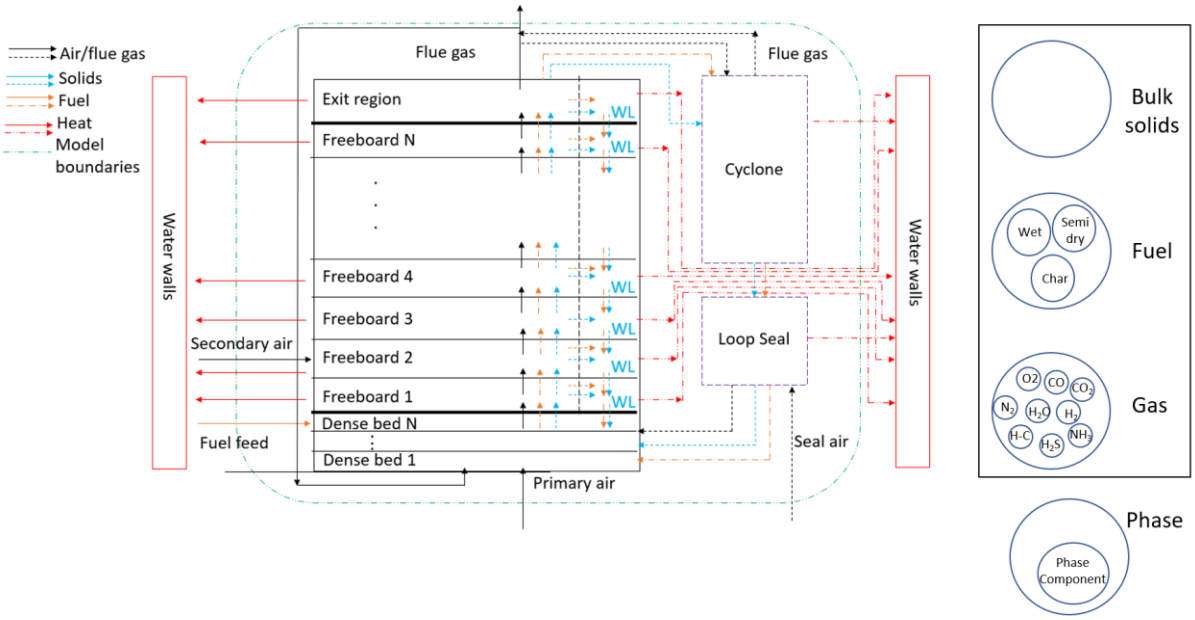

Figure 10. Schematic of the dynamic model of the gas side including domain discretization and scheme of phase and phase components. Dotted lines/arrows are exclusively present in CFB conditions. Source: **Paper I**

4.1.1 Fluid dynamics

In the model, the height of the dense bed is considered to be constant and is selected according to the total riser pressure drop (handled as an input). Note that when the model is run in BFB mode, all of the solid phase is assumed to remain in the bottom bed, i.e., solids entrainment is neglected. When run in the CFB mode, the in-furnace fluid dynamics is a 1.5D description that assumes, based on previous findings [81], that there is no gas flow in the wall-layers. The solids flow is modeled in accordance with previous publications [82], [83], with the solids entrainment from the bottom and the backflow effect at the furnace top being modeled using expressions derived from the data in a previous study [84] [Eqs. (3) and (4), respectively]. The

entrained solids are assumed to flow upwards at their slip velocity, calculated from the single-particle terminal velocity [85], which is also assumed to be the velocity at which the solids flow downwards in the wall-layers [86]. The backmixing of solids to the waterwalls in the freeboard is modeled according to Eq. (5) (solids clusters in the splash zone [80]), and Eqs. (6) and (7) (transfer of the entrained to the walls in the freeboard [82], [84], [87]), respectively. **Paper I** includes a detailed description of how Eqs. (3) – (7) are used in the mass balances of the CFB gas side model.

$$\frac{c_{s,entr} \cdot (u - u_t)}{\rho_g \cdot u} = 3109 \cdot (1 - \frac{u_t}{u})^{6.8} \quad (3)$$

$$k_b = 0.85 \cdot \left[\frac{1}{1+\exp(-66 \cdot St)}\right]^{255} \quad (4)$$

$$a = 4\frac{u_t}{u} \quad (5)$$

$$K = \frac{4k}{D_e(u - u_t)} \quad (6)$$

$$k = 0.1084 \cdot (u - u_t) \quad (7)$$

4.1.2. Fuel conversion

The model accounts for the main steps involved in the conversion of solid fuel particles typical for FB conditions, i.e., drying and devolatilization, and char combustion, using a characteristic time for each. The drying and devolatilization processes are driven by heat transfer and occur simultaneously given the large fuel particle sizes in FBC units, with a combined drying and devolatilization time as a function of the fuel particle size taken from [88]. The time for char combustion is calculated according to the expressions for shrinking sphere conversion regime under transport-controlled conditions. Lastly, the model includes three homogeneous reactions: the combustion of CO, H_2 and light hydrocarbons, with rates calculated according to [89] and [90].

4.1.3. Heat transfer

The formulation of the heat transfer differs between the CFB and BFB modes. Under CFB conditions, bed-to-wall heat transfer in a certain cell *i* is modeled as the combined contributions of convection and radiation, as expressed in Eq. (8). The convective heat transfer coefficient is modeled as a function of the solids concentration in the wall-layers according to [91]. For the radiative contribution, the model introduces the radiation efficiency factor suggested previously [91], according to which the radiation of heat from the core solids to the waterwalls increases as the solids concentration in the freeboard decreases.

$$Q_{extracted,i} = h_c \cdot A_w \cdot (T_{wl} - T_w) + \eta_{rad} \cdot \varepsilon_{susp,i} \cdot A_w \cdot \sigma \cdot (T_c^4 - T_w^4) \quad (8)$$

When run under BFB conditions, the convective heat transfer to the waterwalls is neglected and only radiation is accounted for. This radiative heat transfer shows a relatively low optical thickness in the freeboard of BFB units, which allows the different surfaces to radiate heat to

each other. Thus, the model accounts for radiation between surfaces and volumetric cells, with geometric view factors calculated according to [92] (for details, see **Paper I**). Note that even at the low gas velocities characteristic of BFB operation, the freeboard contains a small amount of fine solids, which are known to influence the emissivity of the volumetric cells. This cell emissivity is computed according to Beer´s law [Eq. 9], where k_{vol} is a tuning factor (see Section 4.3 and **Paper I**) that depends on the gas velocity, in order to account for the contribution of the solids fines at different loads.

$$\varepsilon_{vol} = 1 - e^{-k_{vol}Lp} \tag{9}$$

4.2. Water-steam side

The dynamic process model of the water-steam side is built using the Modelon ThermalPowerLibrary [93]. The different components have been modeled using the lumped parameter approach, which is known to be a valid assumption when describing power plants at the process level [94]. Regarding those components for which such a 0D representation is not appropriate, e.g., a tube, a 1D discretization is applied. For all the components, geometric data were fed into the model according to the design of the reference plant (Section 3.1.2).

In the convection path, the heat transfers on the gas and water-steam sides of the superheaters and economizers are modeled according to Nusselt number correlations from [95], while the evaporator tubes model uses a correlation based on the Dittus-Boelter equation. The wall separating the two sides is modeled as a 1D domain, assuming heat accumulation with a thermal resistance function of the wall thickness, area and conductivity.

The steam drum is modeled according to [96], solving the dynamic energy and mass balances for the liquid and vapor volumes. Heat transfer through the drum walls and heat accumulation in the walls are neglected. The natural circulation of the two-phase flow through the evaporator tubes is modeled with an ideal height difference that yields a certain pressure head.

The steam turbine is described by a quasi-static model, an assumption that is found valid when comparing its characteristic time with those of other plant components such as condensers [97]. The power generation is calculated based on the inlet and outlet steam enthalpies with a constant dry isentropic efficiency [98]. The off-design performance is modeled according to Stodola´s law of cones, according to which the flow area coefficient K_t is calculated as:

$$K_t = \frac{F_n}{\sqrt{p_{i,n}\rho_{i,n}\left(1-\left(\frac{p_{0,n}}{p_{i,n}}\right)^2\right)}} \tag{10}$$

Lastly, the steam condensers are modeled as horizontal cylindrical vessels with a hotwell at the bottom where the condensate is accumulated. The model assumes thermodynamic equilibrium between the two phases. A wall model separates the condensing steam from the cooling fluid, with a heat transfer correlation for condensing steam over horizontal tubes and one based on the logarithmic average of the inlet and outlet temperatures for the cooling media, as derived from [95]. The deaerator is modeled in a similar manner, albeit without cooling tubes and neglecting the heat transfer through the walls.

The supervisory controllers are modeled as PI controllers that are tuned according to the PID tuning rules described by Skogestad [99]. Note that for tuning the supervisory control structures, the regulatory control layer needs to be already tuned and kept in a closed loop. For cascade control loops, the slave controller (i.e., the internal, faster controller) is tuned first.

4.3. Model calibration and validation

4.3.1 Calibration

Due to the assumptions associated with BFB and CFB operation (see Section 4.1), the respective calibrations of the gas-side model are based on different parameters (see Table 5). For CFB conditions, characterized by a large amount of entrained solids in the riser, the model is calibrated by tuning the mean particle diameter of the bulk solids, which differs from the mean size of the fed particles due to particle attrition and size segregation phenomena. For BFB conditions, where the heat transfer to the walls is assumed to be driven exclusively by radiation, the entrainment of miniscule amounts of solids fines is known to have a significant impact on the emissivity of the freeboard cells. As this is a complex mechanism to model, it is here handled as a calibration factor through tuning the effective absorptivity of the freeboard cells, k_g [see Eq. (9)]. Lastly, the gas mixing rate governing the homogeneous reactions is used as a calibration factor in both BFB and CFB operations. Regarding the water-steam side, the present work follows the common practice in dynamic process modeling of calibrating the model by tuning a pre-exponential factor in the correlations for the heat transfer coefficients. The specific values of the tuned calibration factors are discussed and listed in **Papers I** and **III**.

Table 5. Calibration factors used in each of the dynamic models.

			Calibration factors
Gas side	CFB mode	-	Gas mixing
		-	Bulk solids size
	BFB mode	-	Gas mixing
		-	Absorptivity of the gas-solids suspension
Water-steam side		-	Heat transfer correlations

4.3.2 Steady-state operation

The results from the calibration and validation of the gas side are shown in Figure 11, where the heat transfer to the waterwalls computed by the model is compared to those measured in the reference units under steady-state conditions. Note that two datasets at 100% load are used for calibration of the CFB conditions, corresponding to two different fuel conditions. It is evident that the simulated values are in good agreement with the reference plant data, with average errors to the measurements of 1.9% for the calibrated cases and 4.9% for the validation cases. When validating the steady-state operation of the water-steam side, all the errors

between the simulated and measured process variables (e.g., drum pressure, DH outlet temperature or generated power, among others; see **Paper III** for details) remain below 5%, with an average percentage error of 1.5%.

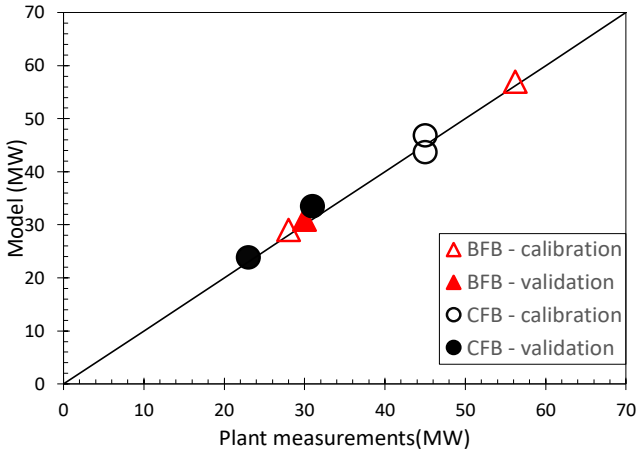

Figure 11. Parity plot comparing the in-furnace heat transferred to the waterwalls computed by the model and measured in the reference plants. Source: **Paper I**

4.3.3 Transient operation

Validation of the transient performances of the models is done by comparing the model output with measurements taken during 2–3 hours of transient operation. Figure 12 shows the input values of the 50→100% load change used for validation of the CFB-CHP plant model. Figure 12a plots the load set-point input into the master load controller, while Figure 12b shows the variations in the DH boundary conditions. The results from the corresponding transient validation are shown in Figure 13, where variables from the gas side (cyclone temperature; Figure 13a) as well as from the water-steam side (DH load and generated power, Figure 13b; and live steam mass flow, Figure 13c) are included. As observed, the model describes rather well the behavior of the reference plant when subjected to a load change. Thus, it can be concluded that the dynamic models are capable of describing with good accuracy the steady-state and transient behaviors of large-scale FBC plants during industrial operation.

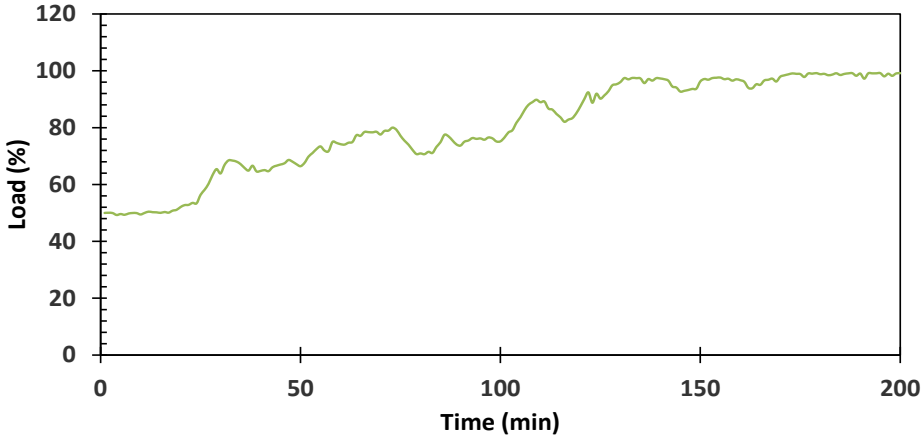

a) Load (%)

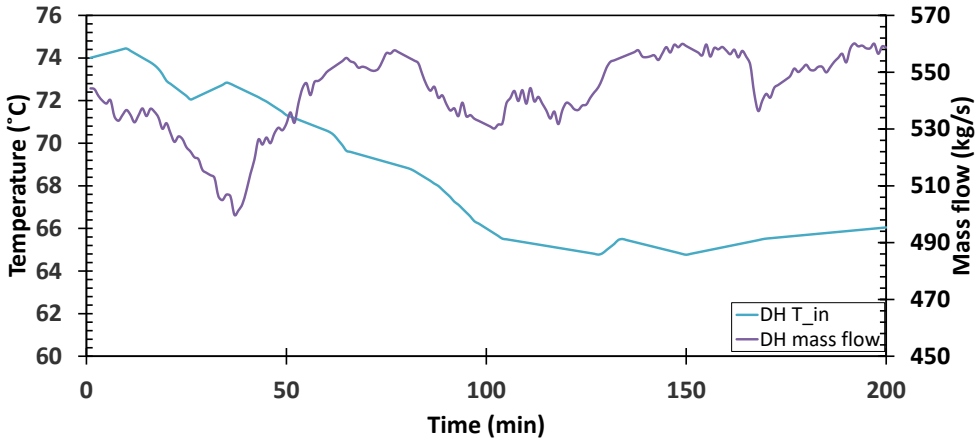

b) DH inlet temperature and mass flow

Figure 12. Input trajectories to the integrated plant model for transient operation validation. Source: **Paper III**

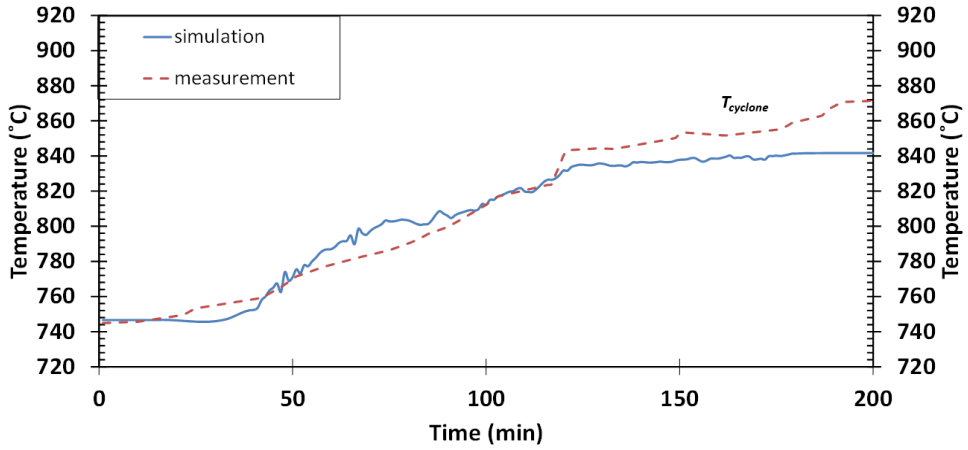

a) $T_{cyclone}$

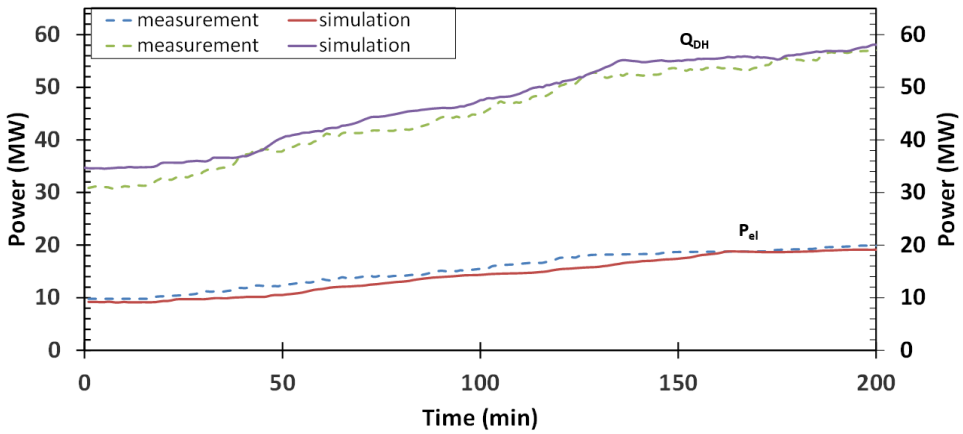

b) Q_{DH} and P_{el}

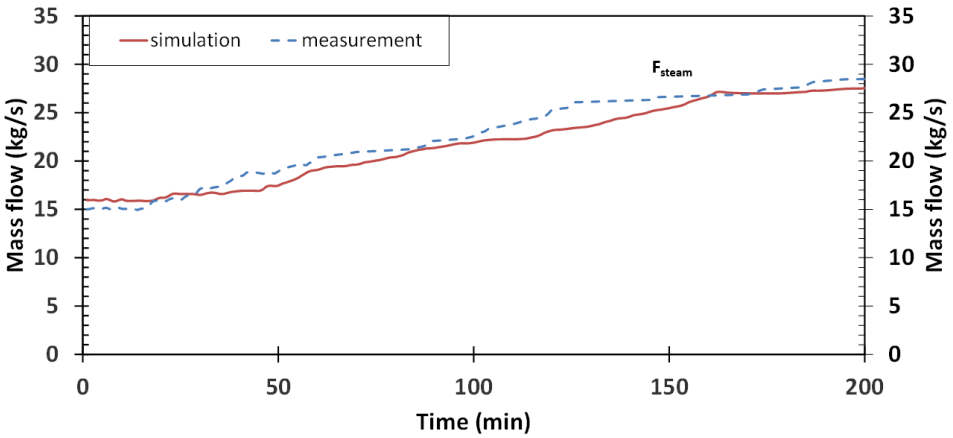

c) F_{steam}

Figure 13. Transient validation of the main process variables of the gas and water-steam sides. The plots compared the simulated and measured trajectories over a 3h load increase for a) cyclone temperature b) DH heat production and generated power and c) mass flow of live steam. Sources: **Paper I** and **III**

5. Selected results and discussion

The most important findings from the three appended papers are presented and discussed in this chapter, the structure of which is aligned with the research questions formulated in Chapter 1. First, the inherent dynamic behaviors of FBC plants are presented, both for the gas side (**Papers I** and **II**) and at the plant (gas and water-steam sides) level (**Paper III**). Second, the performances of FBC plants under different supervisory control strategies are addressed. Lastly, the dynamic interplay between the gas and water-steam sides in FBC plants is discussed.

5.1.Inherent dynamics of FBC plants

5.1.1 Gas side

The inherent dynamics of the gas sides of the CFB and BFB reference furnaces are analyzed and compared in Figure 14. Figure 14, a and b shows the open-loop transient responses of the main process variables of the gas side when the load is reduced in a single step from 100% to 75% in the CFB and BFB, respectively. In the CFB furnace, the bottom temperature is reduced to a lesser extent than the temperature at the top of the furnace because: (i) the dense bed has much larger solids flows than the top of the reactor; and (ii) at lower loads, i.e., at lower gas velocities, the relative content of fuel in the bottom region increases, whereas it decreases in the upper region. Besides, due to the larger heat capacity of the bottom region (consequence of the solids inventory), the temperature response in the bottom region is slower than that at the furnace top. In the BFB furnace (Figure 14b), the differences in heat capacity between the bottom and top regions are more pronounced, which explains the larger differences observed in these regions for the transient responses and the stabilization times of the temperatures.

Figure 14, c–f shows the computed stabilization times (t_s) and relative changes (RC) of the CFB and BFB reference furnaces when the magnitude of the introduced load change is varied. In line with the observations mentioned above, it is evident that the stabilization time of the dense bed is always longer than that at the top of the furnace for all the cases investigated, although the relative change is smaller. Thus, these differences are maximized in the BFB furnace, with the stabilization time in the dense bed being around 20 minutes, compared to 30–100 seconds at the top of the furnace. Another important aspect highlighted in Figure 14, c and e is that when the load is incremented, the stabilization times are significantly shorter than those related to a load reduction of the same magnitude. This aspect, which has been previously reported for other thermal processes (see [43] and [100]) and is explained in detail in **Papers I** and **II**, reflects the fact that a load reduction relies on the heat transfer to the waterwalls, a process that is generally slower than the heat release due to fuel conversion driving the temperature change under a load increase. As shown in Figure 14, the dynamics of the heat transfer to the waterwalls Q_{wall} are largely driven by the in-furnace temperatures, thus stabilization is achieved just before/after the temperature at the furnace top stabilizes.

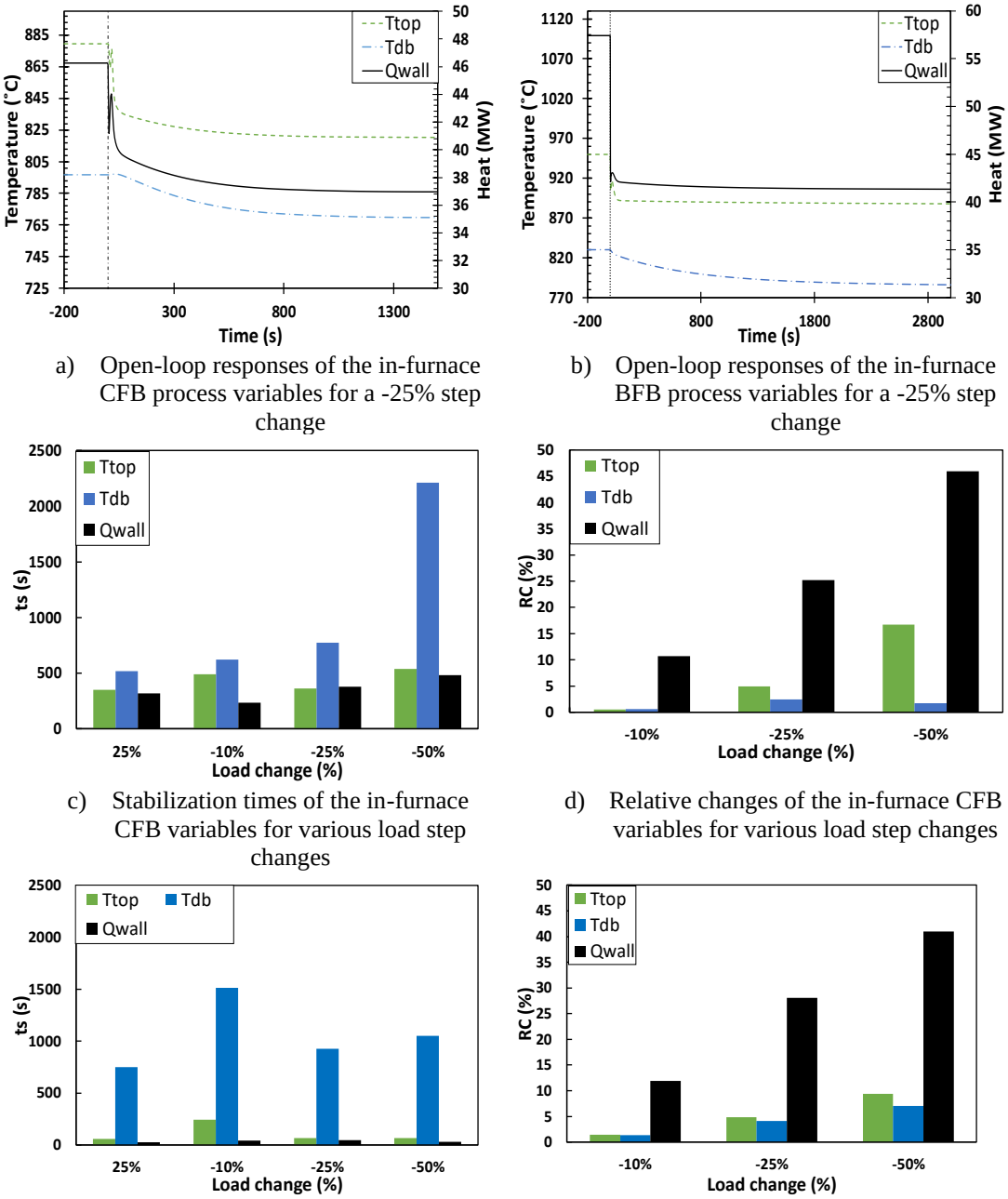

a) Open-loop responses of the in-furnace CFB process variables for a -25% step change

b) Open-loop responses of the in-furnace BFB process variables for a -25% step change

c) Stabilization times of the in-furnace CFB variables for various load step changes

d) Relative changes of the in-furnace CFB variables for various load step changes

e) Stabilization times of the in-furnace BFB variables for various load step changes

f) Relative changes of the in-furnace BFB variables for various load step changes

Figure 14. Inherent dynamics of the gas sides of the reference CFB and BFB furnaces, expressed as variable trajectories, stabilization times (t_s) and relative changes (*RC*). Source: **Paper I**.

To analyze the dependencies of the stabilization times of the gas side on the three main mechanisms taking place in the furnace (fluid dynamics, fuel conversion and heat transfer), additional open-loop tests are performed for the -25% load reduction, whereby the characteristic times of each of the mechanisms (defined and varied as shown in Table 6) are varied independently (for details, see **Paper II**). A representative selection of the runs is plotted in Figure 15a (reference BFB furnace, note the double *y*-axis) and Figure 15b (CFB furnace upscaled to the same thermal capacity as the BFB reference furnace). Table 6 formulates simplified mathematical expressions that relate the stabilization times of the three gas-side

variables monitored (heat extracted from the furnace and temperatures at the furnace bottom and top of the furnace) to the characteristic times of the above-mentioned furnace mechanisms.

Table 6. Characteristic times of the main in-furnace mechanisms of CFB and BFB furnaces. The table shows how these have been varied in the model to evaluate their impacts on the in-furnace dynamics. Note that the fluid dynamics characteristic time of the BFB furnace has not been varied. Source: **Paper II**.

Mechanism	**Characteristic time**		**Variable varied**	
	CFB	BFB	CFB	BFB
Fluid dynamics	$\tau_{FD,CFB} = \tau_{riser} + \tau_{cyclone} + \tau_{loop-seal}$	$\tau_{FD,BFB} = \tau_{gas}$	Size of loop seal (for CFB)	-
Fuel conversion	$\tau_{FC} = t_{char}$		Char conversion time	
Heat transfer	$\tau_{HT} = \frac{\sum M_i C_{p,i}}{\sum F_i C_{p,i}}$		Solids heat capacity	

In agreement with the discussion coupled to Figure 14, the dense bottom bed of the BFB furnace takes much longer to stabilize (600–1500 seconds) than the temperature at the furnace top and the heat extracted through the walls. It can be seen that the stabilization times at the furnace bottom correspond roughly to the sum of the characteristic times of the two mechanisms present in the dense bottom bed, i.e., the fuel conversion and the heat transfer [see Eq. (11)]. In contrast, the temperature at the furnace top and the heat transfer to the walls stabilize in 60–80 seconds and 40–70 seconds, respectively, as a consequence of Q_{wall} being driven by the change in effective gas emissivity forced by the varied presence of solids fines entrained by the gas. Given the very low thermal inertia of the upper regions of the BFB furnace, its temperature dynamic behavior can be expressed as a function of the residence time of the gas triggering the change in gas emissivity, and to a minor extent [see Eq. (12)], the stabilization time of the temperature exiting the bottom region. Since Q_{wall} depends mainly on the gas temperature and effective emissivity, its stabilization time can be approached as that of the temperature at the furnace top [Eq. (13)].

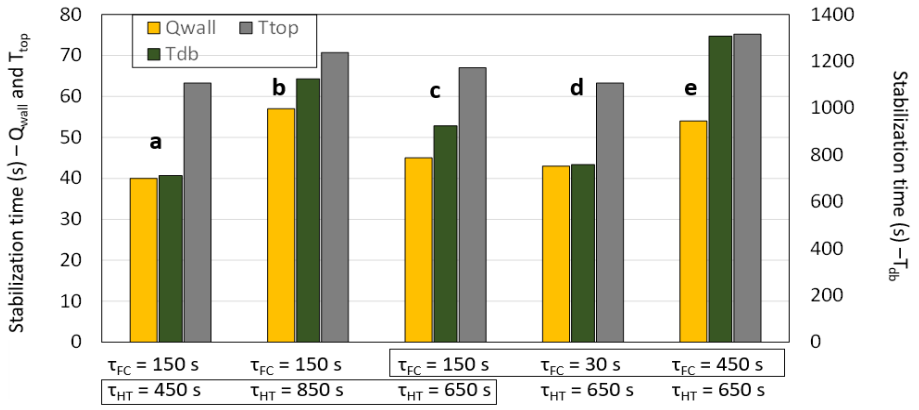

a) BFB furnace

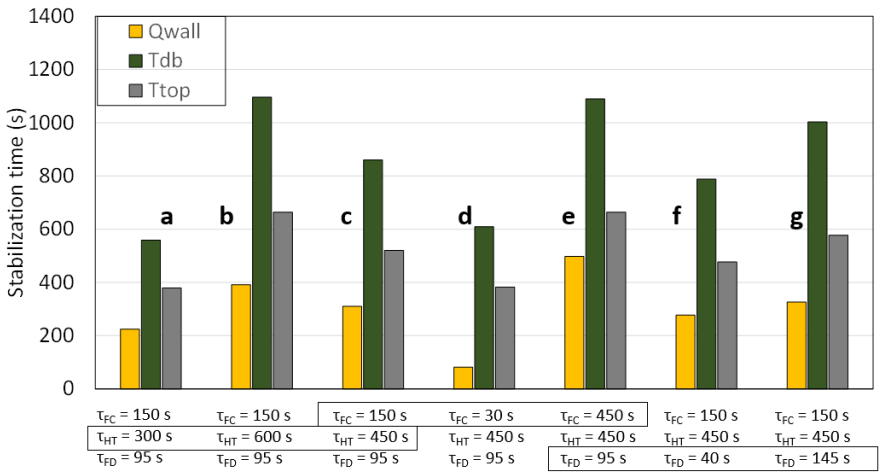

b) CFB furnace

Figure 15. Stabilization times of the gas sides of the BFB and CFB furnaces under variations of the characteristic times of the three in-furnace mechanisms (FC, fuel conversion; FD, fluid dynamics; HT, heat transfer). Note that the characteristic time of FD is not varied in the BFB furnace. Source: **Paper II**.

When analyzing the stabilization times of the monitored variables in the CFB furnace, a relatively uniform effect of the three mechanisms considered for the CFB conditions is observed on the gas-side temperatures. Furthermore, in the bottom region, the stabilization time can be directly approximated as the sum of the three characteristic times [Eq. (14)]. Thus, even though the changes in fluid dynamics, fuel conversion and heat transfer are occurring in parallel, the tails of each of these mechanisms follow each other and add up sequentially to give the total stabilization time. As for the temperature in the upper furnace, its stabilization generally occurs some 30% faster than that at the furnace bottom [Eq. (15)]. Lastly, the dynamics of the heat transfer to the waterwalls are found to be sensitive to all the investigated variations, although they are predominantly influenced by the fuel conversion time [Eq. (16)].

These results may be of importance when assessing the transient capabilities of the gas side of a given FB furnace with a certain size, fuel and bulk solids. The expressions in Table 7 represent a simple way to estimate the impacts of specific changes in the gas velocity, fuel size or composition, or a change in the solids inventory on the dynamic behaviors of key in-furnace variables.

Table 7. Simplified expressions for the dependency of the stabilization times (t_s) of the gas side on the characteristic times of the three in-furnace mechanisms (FC, fuel conversion; FD, fluid dynamics; HT, heat transfer). Source: **Paper II**.

Unit	Variable	Expression	
BFB	T_{db}	$t_{s,DB} \approx \tau_{FC} + \tau_{HT}$	(11)
	T_{top}	$t_{s,top} \approx \tau_{FD} + 0.05\ t_{s,DB}$	(12)
	Q_{wall}	$t_{s,Q} \approx t_{s,top}$	(13)
CFB	T_{db}	$t_{s,DB} \approx \tau_{FC} + \tau_{HT} + \tau_{FD}$	(14)
	T_{top}	$t_{s,top} \approx 0.7\ t_{s,DB}$	(15)
	Q_{wall}	$t_{s,Q} \approx \tau_{FC}\ (0.2\ \tau_{FD} + 0.5\ \tau_{HT})$	(16)

5.1.1 CFB-CHP plant

The computed stabilization times (in minutes) of the main process variables (i.e., generated power, DH production, live steam mass flow, DH outlet temperature, live steam pressure, and in-furnace heat transfer to the walls) when performing open-loop tests in the CFB-CHP plant with step variations of the operational inputs (combustion load, DH flow, DH inlet temperature and fuel heating value) are shown in Figure 16. First, it is evident from comparing Figure 16a (-20% steps) and Figure 16b (+20% steps) that, as occurred within the gas side, the process tends to stabilize faster (on average, 15% shorter stabilization times) when heat is added to the system, i.e., when the combustion load, fuel heating value and DH inlet temperatures are increased. When comparing the stabilization times of the different variables, the live steam pressure and mass flow are found to be the fastest to reach stabilization within the water-steam side, averaging 5 minutes for the investigated cases, which is comparable to the gas-side variable added in Figure 16, i.e., Q_{wall}. The generated power stabilizes within 8 minutes on average, whereas the outlet DH temperature and the condenser heat load are the slowest variables to reach stabilization, with average times of 10 and 13 minutes, respectively. Figure 16 also shows that the process transient response is the fastest to react to changes in the DH mass flow, whereas the disturbances linked to the furnace, i.e., the combustion load and fuel heating value, yield the slowest stabilization times, averaging 11 and 13 minutes, respectively, for the cases investigated.

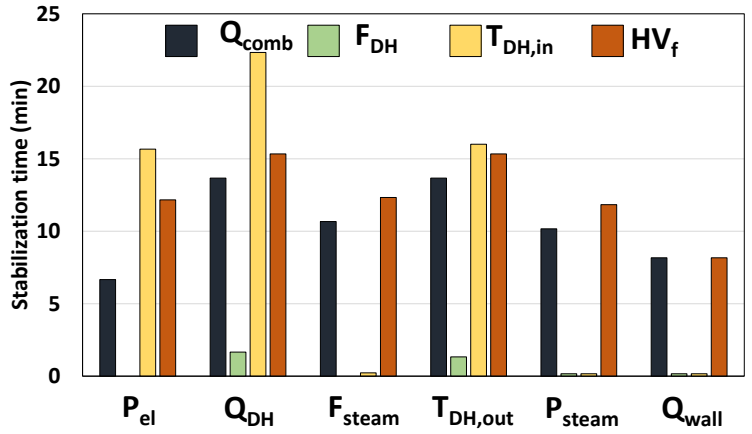

a) -20% step

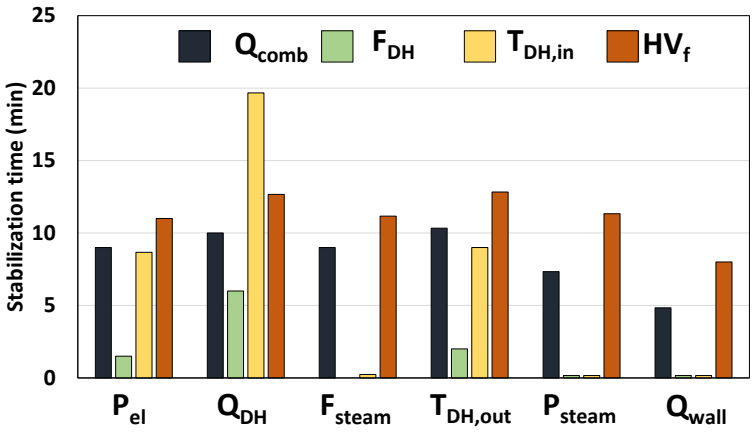

b) +20% step

Figure 16. Inherent dynamics of the CFB-CHP plant, computed as the stabilization times (t_s) of the main process variables for different process disturbances, i.e., step-changes in Q_{comb}, F_{DH}, $T_{DH,\text{in}}$ and HV_f. Source: **Paper III**.

5.2. Controlled dynamics

The simulated trajectories of the power generated by the reference CFB-CHP plant when the load is changed from 100% to 50% at different ramping rates under each of the investigated control strategies are plotted in Figure 17. While Figure 17, a and b (i.e., the slowest ramping rates investigated, at -0.005 and -0.05%/s, respectively) show that for all the tested control strategies, the plant is capable of executing load changes at the same rate as the set-point is varied. Figure 17, c and d (i.e., the fastest ramping rates investigated at -0.5 and -5.0%/s, respectively) present noticeable differences between the control structures. It is clear that the control strategies that manipulate the steam valve opening to regulate the plant load, i.e., Hybrid and BF, provide fast power output changes that are able to follow the set-point. In contrast, the control strategies that manipulate the combustion load, i.e., FP and TF, provide considerably slower load changes, with rising times of 6 minutes and 4 minutes, respectively, and stabilization times of up to 10 minutes. This can be explained by the dynamic effect of the control valve, which uses the energy accumulated in the drum and superheater tubes to generate fast, temporary changes in the steam pressure and flow, which quickly propagate to the turbine. Figure 18 displays the live steam pressure prior to the control valve for the fastest ramping rate

under TF, BF and Hybrid operation. It is clear that the rapid changes in power output provided by the Hybrid and BF strategies are achieved at the expense of steam throttling, caused by fast valve closing. The overshoot in the pressure trajectory is up to +30% for the BF case, as compared for instance to +0.01% for the TF case. This temporary overshoot can be directly linked to exergy losses and, therefore, loss of available work, resulting in a period of low process efficiency that lasts until the pressure is stabilized. Under FP operation, where the steam valve remains fully open during all the operational window, the opposite occurs: although the plant response is considerably slower due to the thermal inertia associated with the gas side, the throttling losses during the process transient response are minimized.

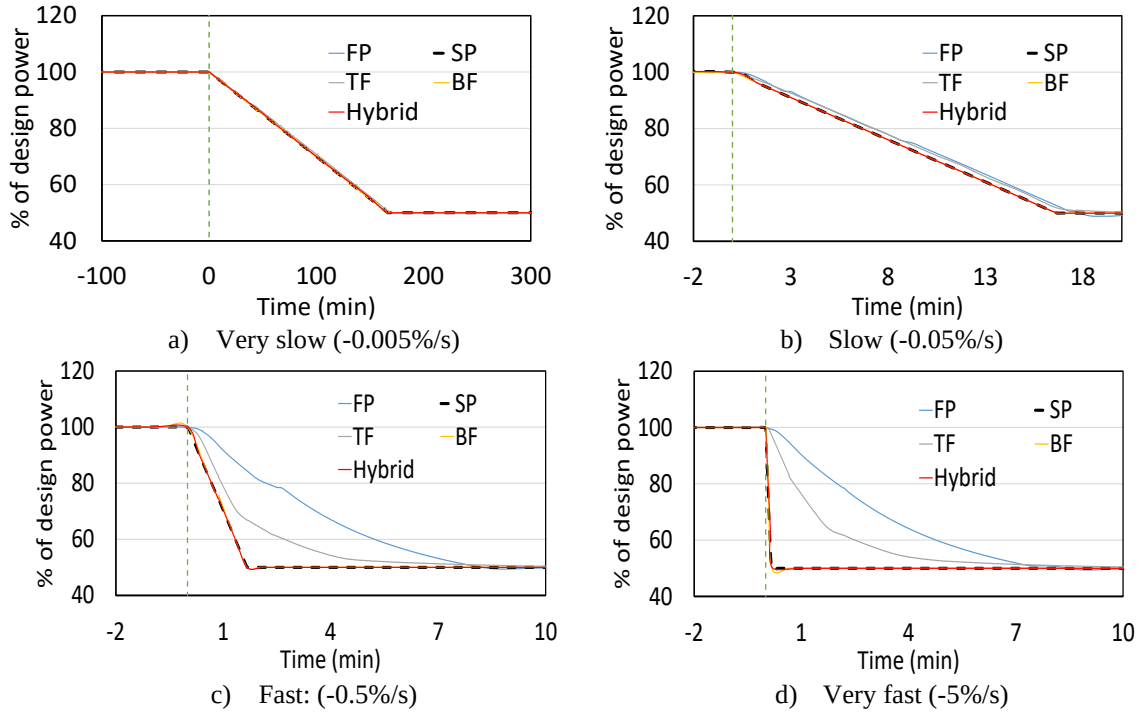

Figure 17. Responses of the generated power (in % of design power) compared to the load set-point (SP) for the 100%→50% load change under different control strategies and ramping rates. FP, Floating pressure; TF, turbine-following; BF, boiler-following. Source: **Paper III**.

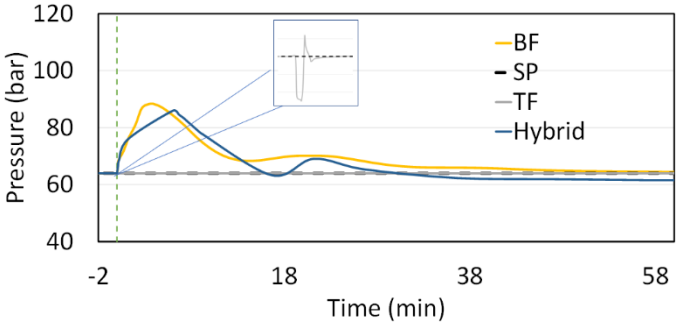

Figure 18. Live steam pressures compared to the set-point (SP) for the very fast (-5.0%/s) ramping rate of the 100%→50% load change. Source: **Paper III**.

5.3.Dynamic interaction between the gas and water-steam sides

Assuming a quasi-static transient behavior for the gas side is a commonly used approach when modeling the dynamics of combustion plants because it yields substantial savings related to the complexity and computational cost of the model. Based on the results obtained in **Papers I–III**, the dynamic interplay between the gas and water-steam sides in large-scale FBC plants can be explored.

Table 8 summarizes the inherent stabilization times computed for the main process variables of the gas and water-steam sides. Table 8 lists only those scenarios that relate to the -20%/-25% load reductions driven by decreases in the fuel input flow. These have been chosen in order to allow for the comparison, since stabilization times increase with the magnitude of the load change (for details, see **Paper I**) and vary depending on the change-driving parameter. Due to the large differences in dynamics between the bottom and top regions of the furnace in BFB units, the stabilization times of the corresponding temperatures in such units are presented separately. It is evident that the stabilization times are of the same order of magnitude in both the gas sides and the water-steam sides of CFB furnaces. In contrast, in BFBs, the relevant in-furnace parameters interfacing with the water-steam side – the heat extracted in the furnace and the flue gas temperature before the convection pass (i.e., the top/outlet furnace temperature) – exhibit dynamics that are one order of magnitude faster than the water-steam side.

Table 8. Summary of the inherent stabilization times of the gas and water-steam sides of the investigated units.

Variable	**Inherent stabilization times (min)**	
Gas side	CFB furnaces	BFB furnaces
Temperatures	3–21	T_{db}: 10–26 T_{top}: 1–1.5
Heat transfer to waterwalls	2–10	0.5–1.0
Water-steam side		
Live steam pressure and mass flow	10	
Power generation	8	
DH temperatures and heat flows	13–15	

Paper I analyzes the responses of the gas side variables when the load change is introduced as a step function and at two different rates that are typical of industrial operation (see Figure 19a). As can be seen in the response trajectories included in Figure 19b, the inherent dynamics observed for the open-loop responses disappear as the rate of the load change is slowed, eventually yielding a ramp-like response for the slowest rate in the temperature at the furnace top and the heat extracted through the furnace walls. This observation indicates that those variables adopt a pseudo-steady-state behavior, i.e., at any time during load ramping, the variables adopt the same values that they would have under steady-state conditions. Generally, this effect arises when the load change is introduced at a rate with a longer characteristic time than the inherent stabilization time of the variable. Note that the temperature in the dense bed, with an inherent stabilization time longer than 600 seconds according to Table 8, does not follow the load ramp and it displays some dynamic behavior well beyond 10 minutes.

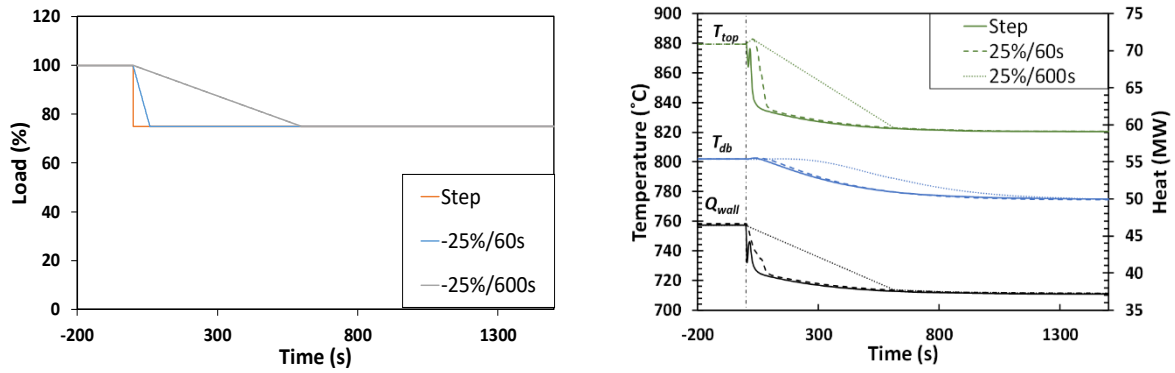

a) Input load changes b) Responses of the CFB furnace

Figure 19. Variable ramping rate (VRR) test in the gas side of the CFB furnace. Source: **Paper I**.

Therefore, it can be concluded that for an accurate prediction of the transient performance of FBC plants, the description of the dynamics of the gas side is crucial, especially when investigating changes over characteristic times that are shorter than the inherent dynamics of the gas side, as well as when the variables of interest are those connected to the live steam. As shown in Table 8, the response times of variables such as the generated power or the live stem pressure are very much reliant on the stabilization times of the gas side which, based on the investigation presented in **Paper II**, are indeed a function of the fuel and bulk solids properties, among other operational conditions. While these findings are of special importance for CFB furnaces, assuming a quasi-static behavior for the gas side might suffice to describe the transient operation of BFB plants.

These results are relevant when assessing the transient capabilities of FBC plants to provide load changes in short timeframes on a regular basis, as needed for instance for primary control reserve (characterized by response times in the order of 30 seconds in most European markets). Furthermore, fast load ramping would yield undesired temporary emissions (as indicated by the results in **Paper I**), highlighting the importance of a dynamic model of the gas side for a robust assessment of the flexibility capabilities of FBC units.

6. Conclusions

This thesis analyzes the dynamic behaviors of commercial-scale fluidized bed combustion plants for heat and power production. The work involves the development and use of mechanistic dynamic models of both the gas and water-steam sides of bubbling and circulating FBCs. Two industrial-scale plants are used to acquire steady-state and transient operational datasets for calibration and validation of the models, as they are used as reference cases for the performed dynamic analyses.

With respect to the analyses of the inherent dynamics of FBC plants, the following can be concluded:

- Evaluation of the impact of the thermal inertia created by the bulk solids on the in-furnace dynamics of FBC plants reveals that regions with large heat capacities, such as the bottom of the furnace in BFB units, take up to 10-times longer to stabilize than does the furnace top. CFB furnaces show a more even distribution of solids throughout the furnace, which yields stabilization times that are more similar across the different regions. While the stabilization times of the gas sides of CFB combustors are found to be dependent upon the characteristic times of the main in-furnace mechanisms (i.e., fuel conversion, heat transfer and fluid dynamics), the dynamics of BFB units are driven mainly by the residence time of the gas. For this reason, the heat transferred to the waterwalls displays faster transient responses in BFB units than in CFB combustors.
- Due to reduced residence time of the gas and water-steam flows, FBC plants respond faster to changes when running at higher loads. In addition, changes which imply a heat removal from the system (e.g. decreasing combustion or DH load or increasing the fuel moisture) leads to slower transients than the inverse.
- Lastly, it can be concluded that although the dynamic behaviors of the gas sides of FBC plants can be assumed to be quasi-static when operated at rates that are typical of heat-driven operation, dynamic modeling of the gas side is critical for accurate prediction of the process dynamics when assessing faster operation. This aspect attains greater importance in CFB combustors because the in-furnace transients are found to be of the same magnitude as those of the water-steam side, while the in-furnace responses of BFB units are found to be one order of magnitude faster than those of the water-steam side.

Regarding control and operational strategies to improve the operational flexibility of FBC plants, the following is concluded:

- Implementing supervisory control strategies can have a strong positive impact on maximizing the load change capabilities of FBC plants. While control strategies for load changes based on modifying the fuel input flow can provide changes in the order of 5%/min, strategies that manipulate the live steam control valve can follow changes in generated electricity at rates as fast as -5%/s. The results show that the increased ramping capabilities offered by these strategies come at the expense of lowered thermal efficiency due to steam throttling, revealing a trade-off between flexibility and efficiency, as well as the need for economic optimization.

Furthermore, other constraints must be considered when assessing the transient operation capabilities of FBC plants, such as thermal stresses in key components, undesired pollutant emissions, and the dynamics of subsystems outside the scope of this work (e.g., the fuel handling system).

6.1. Further work

Based on the outcomes and findings of this thesis, new research tasks can be proposed that would likely further our understanding of the transient operational capabilities of large-scale FB units, some of which are listed below.

- As the demand for biofuels increases and the yearly-average capacity utilization of conventional FB boilers remains at low levels (23%-40% in Sweden, depending on the supply side – district heating or industry), the retrofit of FBC plants into polygeneration facilities represents a promising alternative way for FBCs to promote their standing as a key technology for the transition towards a sustainable energy system. It is foreseen that in such a scenario, the dynamic interplay between heat, power and gas production will be crucial for maximizing plant utilization, for understanding the plant capabilities to operate in specific power markets, and for establishing its role as a variation management tool for the electricity system. The dynamic models developed in this thesis could be adapted to account for the retrofits and could subsequently be used to investigate the transient operation capabilities of these facilities.

- The use of large-scale FB reactors for thermochemical energy storage (TCES) through the cycling of solid systems, such as carbonates and redox metals, is gaining global recognition as an efficient storage technology with possibilities in relation to energy shipping. If deployed in a renewable energy generation facility, such as a wind farm or a concentrated solar power (CSP) plant, the transient capabilities of the process would play a crucial role in the effective deployment of the technology. Moreover, advanced control structures could enhance the transient performance of the process, optimizing the operation for the timescales required by the system. Thus, the dynamic models developed in this work and the insights acquired on the dynamics of large-scale FB reactors are valuable for investigating TCES processes based on solids cycling.

- Using model order reduction methods, the high-fidelity models developed in this thesis could be reduced to simpler models that are capable of describing the transient operation of the plants at a much lower computational cost. These simpler models, after verification and validation, could be used to develop model predictive control (MPC) strategies for advanced and robust process control.

References

[1] UNFCCC, "Paris Agreement," *Conf. Parties its twenty-first Sess.*, no. December, p. 32, 2015, doi: FCCC/CP/2015/L.9/Rev.1.

[2] Artur Runge and E. C. Metzger, "A Clean Planet for all Vision for a Clean Planet by 2050," *Eur. Comm.*, no. November, p. 393, 2018.

[3] European Commission, "Roadmap 2050," *Policy*, no. April, pp. 1–9, 2012, doi: 10.2833/10759.

[4] International Energy Agency, "Renewables 2019," 2019.

[5] International Renewable Energy Agency, *IRENA (2019), Global Energy Transformation: A Roadmap to 2050*. 2019.

[6] IEA, "World Energy Outlook (2020)," Paris, 2020.

[7] M. de Groot, W. Crijns-Graus, and R. Harmsen, "The effects of variable renewable electricity on energy efficiency and full load hours of fossil-fired power plants in the European Union," *Energy*, vol. 138, pp. 575–589, 2017, doi: 10.1016/j.energy.2017.07.085.

[8] M. A. Gonzalez-Salazar, T. Kirsten, and L. Prchlik, "Review of the operational flexibility and emissions of gas- and coal-fired power plants in a future with growing renewables," *Renew. Sustain. Energy Rev.*, vol. 82, no. July 2017, pp. 1497–1513, 2018, doi: 10.1016/j.rser.2017.05.278.

[9] J. Beiron, R. M. Montañés, F. Normann, and F. Johnsson, "Flexible operation of a combined cycle cogeneration plant – A techno-economic assessment," *Appl. Energy*, vol. 278, no. August, p. 115630, 2020, doi: 10.1016/j.apenergy.2020.115630.

[10] L. Göransson, M. Lehtveer, E. Nyholm, M. Taljegard, and V. Walter, "The benefit of collaboration in the North European electricity system transition—System and sector perspectives," *Energies*, vol. 12, no. 24, 2019, doi: 10.3390/en12244648.

[11] J. Koornneef and M. Junginger, "Development of fluidized bed combustion — An overview of trends , performance and cost," *Prog. Energy Combust. Sci.*, vol. 33, pp. 19–55, 2007, doi: 10.1016/j.pecs.2006.07.001.

[12] P. Basu, *Circulating fluidized bed boilers: Design, operation and maintenance*. 2015.

[13] M. Gao, F. Hong, and J. Liu, "Investigation on energy storage and quick load change control of subcritical circulating fluidized bed boiler units," *Appl. Energy*, vol. 185, pp. 463–471, 2017, doi: 10.1016/j.apenergy.2016.10.140.

[14] H. Zhang, M. Gao, F. Hong, J. Liu, and X. Wang, "Control-oriented modelling and investigation on quick load change control of subcritical circulating fluidized bed unit," *Appl. Therm. Eng.*, vol. 163, no. September, p. 114420, 2019, doi: 10.1016/j.applthermaleng.2019.114420.

[15] K. Atsonios, A. Nesiadis, N. Detsios, K. Koutita, N. Nikolopoulos, and P. Grammelis, "Review on dynamic process modeling of gasification based biorefineries and bio-based heat & power plants," *Fuel Process. Technol.*, vol. 197, no. March 2019, p. 106188, 2020, doi: 10.1016/j.fuproc.2019.106188.

[16] F. Johnsson, H. Thunman, and D. Pallarès, "Future applications of circulating fluidized-bed technology," in *CFB-13*, 2021, pp. 26–35.

[17] Z. Guo, Q. Wang, M. Fang, Z. Luo, and K. Cen, "Thermodynamic and economic analysis of polygeneration system integrating atmospheric pressure coal pyrolysis technology with circulating fluidized bed power plant," *Appl. Energy*, vol. 113, pp. 1301–1314, 2014, doi:

10.1016/j.apenergy.2013.08.086.

[18] C. Heinze, J. May, J. Peters, J. Ströhle, and B. Epple, “Techno-economic assessment of polygeneration based on fluidized bed gasification,” *Fuel*, vol. 250, no. February, pp. 285–291, 2019, doi: 10.1016/j.fuel.2019.04.020.

[19] G. Zsembinszki, A. Sole, C. Barreneche, C. Prieto, A. I. Fernández, and L. F. Cabeza, “Review of reactors with potential use in thermochemical energy storage in concentrated solar power plants,” *Energies*, vol. 11, no. 9, 2018, doi: 10.3390/en11092358.

[20] S. Padula, C. Tregambi, R. Solimene, R. Chirone, M. Troiano, and P. Salatino, “A novel fluidized bed ‘ thermochemical battery ’ for energy storage in concentrated solar thermal technologies,” *Energy Convers. Manag.*, vol. 236, p. 113994, 2021, doi: 10.1016/j.enconman.2021.113994.

[21] G. Martinez Castilla, D. C. Guio-Perez, S. Papadokonstantakis, D. Pallarès, and F. Johnsson, “Techno-economic assessment of calcium looping for thermochemical energy storage with CO2 capture,” *Energies*, vol. accepted f, 2021.

[22] N. Kumar, S. Besuner, S. Lefton, D. Agan, and D. Hilleman, “Power plant cycling costs,” Sunnyvale, California, 2012.

[23] L. Göransson, J. Goop, M. Odenberger, and F. Johnsson, “Impact of thermal plant cycling on the cost-optimal composition of a regional electricity generation system,” *Appl. Energy*, vol. 197, pp. 230–240, 2017, doi: 10.1016/j.apenergy.2017.04.018.

[24] W. L. Luyben, *Plantwide dynamic simulators in chemical processing and control*. New York: Marcel Dekker, 2002.

[25] F. Alobaid, N. Mertens, R. Starkloff, T. Lanz, C. Heinze, and B. Epple, “Progress in dynamic simulation of thermal power plants,” *Prog. Energy Combust. Sci.*, vol. 59, pp. 79–162, 2017, doi: 10.1016/j.pecs.2016.11.001.

[26] A. Gómez-Barea and B. Leckner, “Modeling of biomass gasification in fluidized bed,” *Prog. Energy Combust. Sci.*, vol. 36, no. 4, pp. 444–509, 2010, doi: 10.1016/j.pecs.2009.12.002.

[27] I. Avagianos, D. Rakopoulos, S. Karellas, and E. Kakaras, “Review of Process Modeling of Solid-Fuel Thermal Power Plants for Flexible and Off-Design Operation,” *Energies*, vol. 13, no. 6587, 2020, doi: doi:10.3390/en13246587.

[28] R. M. Montañés, “Transient performance of combined cycle power plant with absorption based post-combustion CO2 capture: dynamic simulations and pilot plant testing,” NTNU, 2018.

[29] A. P. Under, T. H. E. Clean, and E. Ministerial, “Thermal Power Plant Flexibility.”

[30] J. Beiron, R. M. Montañés, and F. Normann, “Operational Flexibility of Combined Heat and Power Plant With Steam Extraction Regulation,” in *Proceedings of 11th International Conference on Applied Energy*, 2019, pp. 1–4.

[31] E. Mollenhauer, A. Christidis, and G. Tsatsaronis, “Increasing the Flexibility of Combined Heat and Power Plants With Heat Pumps and Thermal Energy Storage,” vol. 140, no. February, pp. 1–8, 2018, doi: 10.1115/1.4038461.

[32] P. Li, H. Wang, Q. Lv, and W. Li, “Combined heat and power dispatch considering heat storage of both buildings and pipelines in district heating system for wind power integration,” *Energies*, vol. 10, no. 7, 2017, doi: 10.3390/en10070893.

[33] D. Romanchenko, J. Kensby, M. Odenberger, and F. Johnsson, “Thermal energy storage in district heating: Centralised storage vs. storage in thermal inertia of buildings,” *Energy Convers. Manag.*, vol. 162, no. January, pp. 26–38, 2018, doi: 10.1016/j.enconman.2018.01.068.

[34] M. Liu, S. Wang, Y. Zhao, H. Tang, and J. Yan, “Heat–power decoupling technologies for coal-fired CHP plants: Operation flexibility and thermodynamic performance,” *Energy*, vol. 188, p. 116074, 2019, doi: 10.1016/j.energy.2019.116074.

[35] K. Laursen and J. R. Grace, “Some implications of co-combustion of biomass and coal in a fluidized bed boiler,” *Fuel Process. Technol.*, vol. 76, no. 2, pp. 77–89, 2002, doi: 10.1016/S0378-3820(02)00021-8.

[36] W. L. I, “CONTROL iOR FlitI m CHEMICAL ENGINEERS SECOND EDITION- a I,” *Pet. Refin. Eng.*

[37] S. Stultz and J. Kitto, “Controls for Fossil Fuel-Fired Steam Generating Plants,” in *Steam: its generation and use*, The Babcok and Wilcox Company, 2005, pp. 41–1, 41–21.

[38] S. Skogestad and I. Postlethwaite, *Multivariable Feedback Control. Analysis and design*. Wiley, 2006.

[39] P. Basu, “Combustion of coal in circulating fluidized-bed boilers: A review,” *Chem. Eng. Sci.*, vol. 54, no. 22, pp. 5547–5557, 1999, doi: 10.1016/S0009-2509(99)00285-7.

[40] M. Richter, G. Oeljeklaus, and K. Görner, “Improving the load flexibility of coal-fired power plants by the integration of a thermal energy storage,” *Appl. Energy*, vol. 236, no. October 2018, pp. 607–621, 2019, doi: 10.1016/j.apenergy.2018.11.099.

[41] E. Oko and M. Wang, “Dynamic modelling , validation and analysis of coal-fired subcritical power plant,” *FUEL*, vol. 135, pp. 292–300, 2014, doi: 10.1016/j.fuel.2014.06.055.

[42] A. Benato, A. Stoppato, and A. Mirandola, “Dynamic behaviour analysis of a three pressure level heat recovery steam generator during transient operation,” *Energy*, vol. 90, pp. 1595–1605, 2015, doi: 10.1016/j.energy.2015.06.117.

[43] R. M. Montañés, S. GarÐarsdóttir, F. Normann, F. Johnsson, and L. O. Nord, “Demonstrating load-change transient performance of a commercial-scale natural gas combined cycle power plant with post-combustion CO2capture,” *Int. J. Greenh. Gas Control*, vol. 63, no. May, pp. 158–174, 2017, doi: 10.1016/j.ijggc.2017.05.011.

[44] F. Alobaid *et al.*, “Dynamic simulation of a municipal solid waste incinerator,” *Energy*, vol. 149, pp. 230–249, 2018, doi: 10.1016/j.energy.2018.01.170.

[45] J. Beiron, R. M. Montañés, F. Normann, and F. Johnsson, “Dynamic modeling for assessment of steam cycle operation in waste-fired combined heat and power plants Absolute Percentage Deviation,” *Energy Convers. Manag.*, vol. 198, no. August, p. 111926, 2019, doi: 10.1016/j.enconman.2019.111926.

[46] A. Cammi, F. Casella, M. E. Ricotti, and F. Schiavo, “An object-oriented approach to simulation of IRIS dynamic response,” *Prog. Nucl. Energy*, vol. 53, no. 1, pp. 48–58, 2011, doi: 10.1016/j.pnucene.2010.09.004.

[47] R. M. Montañés, J. Windahl, J. Pålsson, and M. Thern, “Dynamic Modeling of a Parabolic Trough Solar Thermal Power Plant with Thermal Storage Using Modelica,” *Heat Transf. Eng.*, vol. 39, no. 3, pp. 277–292, 2018, doi: 10.1080/01457632.2017.1295742.

[48] P. J. Dechamps, “Modelling the transient behavior of combined cycle plants,” *Proc. ASME Turbo Expo*, vol. 4, 1994, doi: 10.1115/94GT238.

[49] P. J. Dechamps, “Modelling the transient behaviour of heat recovery steam generators,” *Proc. Inst. Mech. Eng. Part A J. Power Energy*, pp. 265–273, 1995, doi: https://doi.org/10.1243/PIME_PROC_1995_209_005_01.

[50] J. Sandberg, R. B. Fdhila, E. Dahlquist, and A. Avelin, “Dynamic simulation of fouling in a circulating fluidized biomass-fired boiler,” *Appl. Energy*, vol. 88, no. 5, pp. 1813–1824, 2011,

doi: 10.1016/j.apenergy.2010.12.006.

[51] M. Zlatkovikj, V. Zaccaria, I. Aslanidou, and K. Kyprianidis, “Simulation study for comparison of control structures for BFB biomass boiler,” no. September, 2020.

[52] S. Suojanen, E. Hakkarainen, M. Tähtinen, and T. Sihvonen, “Modeling and analysis of process configurations for hybrid concentrated solar power and conventional steam power plants,” *Energy Convers. Manag.*, vol. 134, pp. 327–339, 2017, doi: 10.1016/j.enconman.2016.12.029.

[53] C. K. Park and P. Basu, “A model for prediction of transient response to the change of fuel feed rate to a circulating fluidized bed boiler furnace,” *Chem. Eng. Sci.*, vol. 52, no. 20, pp. 3499–3509, 1997, doi: 10.1016/S0009-2509(97)00128-0.

[54] Y. Majanne and P. Köykkä, “Dynamic model of a circulating fluidized bed boiler,” *IFAC Proc. Vol.*, vol. 42, no. 9, pp. 255–260, 2009, doi: 10.3182/20090705-4-SF-2005.00046.

[55] B. Deng, M. Zhang, L. Shan, G. Wei, J. Lyu, and H. Yang, “Modeling study on the dynamic characteristics in the full-loop of a 350 MW supercritical CFB boiler under load regulation,” *J. Energy Inst.*, vol. 97, pp. 117–130, 2021, doi: 10.1016/j.joei.2021.04.014.

[56] Y. Chen and G. Xiaolong, “Dynamic modeling and simulation of a 410 t/h Pyroflow CFB boiler,” *Comput. Chem. Eng.*, vol. 31, no. 1, pp. 21–31, 2006, doi: 10.1016/j.compchemeng.2006.04.006.

[57] S. Kim, S. Choi, J. Lappalainen, and T. H. Song, “Dynamic simulation of the circulating fluidized bed loop performance under the various operating conditions,” *Proc. Inst. Mech. Eng. Part A J. Power Energy*, vol. 233, no. 7, pp. 901–913, 2019, doi: 10.1177/0957650919838111.

[58] J. Ritvanen, J. Kovacs, S. Mikko, M. Hultgren, A. Tourunen, and T. Hyppänen, “1-d dynamic simulation study of oxygen fired coal combustion in pilot and large scale CFB boilers.”

[59] A. Tourunen, J. Hämäläinen, T. Hyppänen, J. Saastamoinen, K. Paakkinen, and A. Kettunen, “Study of operation of a pilot CFB-reactor in dynamic conditions,” in *17th International Fluidized Bed Combustion Conference*, 2003.

[60] J. Peters, F. Alobaid, and B. Epple, “Operational flexibility of a CFB furnace during fast load change-experimental measurements and dynamic model,” *Appl. Sci.*, vol. 10, no. 17, 2020, doi: 10.3390/app10175972.

[61] D. Stefanitsis, A. Nesiadis, and K. Koutita, “Simulation of a CFB Boiler Integrated With a Thermal Energy Storage System During Transient Operation,” vol. 8, no. September, pp. 1–14, 2020, doi: 10.3389/fenrg.2020.00169.

[62] J. Lappalainen, A. Tourunen, H. Mikkonen, M. Hänninen, and J. Kovács, “Modelling and dynamic simulation of a supercritical, oxy combustion circulating fluidized bed power plant concept-Firing mode switching case,” *Int. J. Greenh. Gas Control*, vol. 28, pp. 11–24, 2014, doi: 10.1016/j.ijggc.2014.06.015.

[63] J. Haus, E. U. Hartge, S. Heinrich, and J. Werther, “Dynamic flowsheet simulation of gas and solids flows in a system of coupled fluidized bed reactors for chemical looping combustion,” *Powder Technol.*, vol. 316, pp. 628–640, 2017, doi: 10.1016/j.powtec.2016.12.022.

[64] J. Findejs, V. Havlena, J. Jech, and D. Pachner, “Model based control of the circulating fluidized bed boiler,” *IFAC Proc. Vol.*, vol. 42, no. 9, pp. 44–49, 2009, doi: 10.3182/20090705-4-SF-2005.00010.

[65] T. Kataja, P. O. Box, F.- Tampere, P. O. Box, and F.- Tampere, “Dynamic Model of a Bubbling Fluidized Bed Boiler,” pp. 140–149.

[66] N. Selçuk and E. Degirmenci, “Dynamic Simulation of Fluidized Bed Combustors and its Validation Against Measurements Dynamic Simulation of Fluidized Bed Combustors and its

Validation Against Measurements," vol. 2202, 2007, doi: 10.1080/00102200108952175.

[67] A. Galgano, P. Salatino, S. Crescitelli, F. Scala, and P. L. Maffettone, "A model of the dynamics of a fluidized bed combustor burning biomass," *Combust. Flame*, vol. 140, no. 4, pp. 371–384, 2005, doi: 10.1016/j.combustflame.2004.12.006.

[68] M. Hultgren, E. Ikonen, and J. Kova, "Once-through Circulating Fluidized Bed Boiler Control Design with the Dynamic Relative Gain Array and Partial Relative Gain," 2017, doi: 10.1021/acs.iecr.7b03259.

[69] M. Hultgren and E. Ikonen, "Integrated control and process design for improved load changes in fluidized bed boiler steam path," vol. 199, pp. 164–178, 2019, doi: 10.1016/j.ces.2019.01.025.

[70] S. Kim, S. Choi, and T. Song, "Dynamic simulation study of the steam temperature in a ultra-supercritical circulating fluidized bed boiler system," vol. 0, no. 0, pp. 1–15, 2020, doi: 10.1177/0957650920915304.

[71] N. Zimmerman, K. Kyprianidis, and C.-F. Lindberg, "Waste Fuel Combustion: Dynamic Modeling and Control," *Processes*, vol. 6, no. 11, p. 222, 2018, doi: 10.3390/pr6110222.

[72] "Karlstad Energi homepage," 2020. [Online]. Available: https://www.karlstadsenergi.se/.

[73] Modelica Association, "Modelica and the Modelica Association — Modelica Association," 1996. [Online]. Available: https://www.modelica.org/.

[74] E. Hairer and G. Wanner, "Stiff differential equations solved by Radau methods," *J. Comput. Appl. Math.*, vol. 111, no. 1–2, pp. 93–111, 1999, doi: 10.1016/S0377-0427(99)00134-X.

[75] C. Zhang, Y. Li, H. Wang, B. A. O. Zhang, F. E. I. Xie, and Y. U. Huang, "Selection of the optimal steam pressure for coal-fired power units," *ICMLC*, no. August, pp. 1835–1838, 2005.

[76] S. Sengupta, A. Datta, and S. Duttagupta, "Exergy analysis of a coal-based 210 MW thermal power plant," *Internatinal J. Energy Res.*, no. April 2006, pp. 14–28, 2007, doi: 10.1002/er.

[77] D. Seborg, T. Edgar, D. Mellichamp, and F. Doyle, *Process dynamics and control*. John Wiley & Sons, 2011.

[78] U. Lackermeier and J. Werther, "Flow phenomena in the exit zone of a circulating fluidized bed," *Chem. Eng. Process.*, vol. 41, pp. 771–783, 2002.

[79] F. Johnsson, A. Vrager, T. Tiikma, and B. Leckner, "Solids flow pattern in the exit region of a CFB-furnace. Influence of geometry," in *Proceedings of the 15th international con- ference on fluidized bed combustion*, 1999.

[80] F. Johnsson and B. Leckner, "Vertical distribution of solids in a CFB-furnace," in *13th International conference on fluidized-bed combustion*, 1995, p. 719.

[81] J. Sterneus and F. Johnsson, "Gas mixing in the wall layer of a CFB boiler," in *Proceedings of the 14th International conference on fluidized bed combustion*, 1997, pp. 1237–46.

[82] F. Johnsson, W. Zhang, and B. Leckner, "Characteristics of the formation of particle wall layers in CFB boilers," in *2nd Int. Conf. on Multiphase Flow, Vol 3*, 1995.

[83] A. Johansson, F. Johnsson, and B. Leckner, "Solids back-mixing in CFB boilers," *Chem. Eng. Sci.*, vol. 62, no. 1–2, pp. 561–573, 2007, doi: 10.1016/j.ces.2006.09.021.

[84] T. Djerf, D. Pallarès, and F. Johnsson, "Solids flow patterns in large-scale Circulating Fluidised Bed boilers: Experimental evaluation under fluid-dynamically down-scaled conditions," *Chem. Eng. Sci.*, vol. 231, p. 116309, 2020, doi: 10.1016/j.ces.2020.116309.

[85] D. Kunii and O. Levenspiel, *Fluidization Engineering*. Butterworth-Heineman, 1991.

[86] W. Zhang, F. Johnsson, and B. Leckner, “Fluid dynamic boundary layers in CFB boilers,” *Chem. Eng. Sci.*, vol. 50, no. 2, pp. 201–210, 1995.

[87] H. Yang, G. Yue, X. Xiao, J. Lu, and Q. Liu, “1D modeling on the material balance in CFB boiler,” *Chem. Eng. Sci.*, vol. 60, no. 20, pp. 5603–5611, 2005, doi: 10.1016/j.ces.2005.04.081.

[88] S. Oka, *Fluidized bed combustion*. New York, 2004.

[89] Flagan;Seinfeld, *Fundamentals of air pollution engineering*. Prentice Hall, 1988.

[90] F. L. Dryer and C. K. Westbrook, “Simplified Reaction Mechanisms for the Oxidation of Hydrocarbon Fuels in Flames,” *Combust. Sci. Technol.*, vol. 27, no. 1–2, pp. 31–43, 1981, doi: 10.1080/00102208108946970.

[91] C. Breitholtz, B. Leckner, and A. P. Baskakov, “Wall average heat transfer in CFB boilers,” *Powder Technol.*, vol. 120, no. 1–2, pp. 41–48, 2001, doi: 10.1016/S0032-5910(01)00345-X.

[92] J. R. Howell, *A catalog of radiation configuration factors*. McGraw-Hill, 1982.

[93] Modelon AB, “Modelon Home,” 2018. [Online]. Available: https://www.modelon.com/.

[94] J. Eborn, “On model libraries for thermo-hydraulic applications,” *Dep. Autom. Control. Lund Inst. Technol.*, p. 135, 2001.

[95] Springer, Ed., *VDI Wärmeatlas*, 9th Editio. Springer, 1997.

[96] F. Casella and A. Leva, “Modelica open library for power plant simulation: design and experimental validation,” *Proc. 3rd Int. Model. Conf.*, no. December, pp. 41–50, 2003.

[97] R. Paranjape, “Modeling and control of a supercritical coal fired boiler,” Texas Tech University, 1996.

[98] R. Beebe, “Condition monitoring of steam turbines by performance analysis,” *J. Qual. Maint. Eng.*, vol. 9, no. 2, pp. 102–112, 2003, doi: 10.1108/13552510310482361.

[99] S. Skogestad, “Probably the best simple PID tuning rules in the world,” in *AIChE Annual Meeting*, 2001, no. November 2001.

[100] G. Martinez Castilla, M. Biermann, R. M. Montañés, F. Normann, and F. Johnsson, “Integrating carbon capture into an industrial combined-heat-and-power plant: performance with hourly and seasonal load changes,” *Int. J. Greenh. Gas Control*, vol. 82, no. January, pp. 192–203, 2019, doi: 10.1016/j.ijggc.2019.01.015.